

Purdue University
Purdue e-Pubs

College of Technology Masters Theses

College of Technology Theses and Projects

3-5-2010

Using Piezoelectric Generation To Harvest Energy From Turbulent Air Flow

Joshua M. Nelson

Purdue University - Main Campus, jmnelson@purdue.edu

Follow this and additional works at: <http://docs.lib.purdue.edu/techmasters>

Nelson, Joshua M., "Using Piezoelectric Generation To Harvest Energy From Turbulent Air Flow" (2010). *College of Technology Masters Theses*. Paper 2.

<http://docs.lib.purdue.edu/techmasters/2>

This document has been made available through Purdue e-Pubs, a service of the Purdue University Libraries. Please contact epubs@purdue.edu for additional information.

PURDUE UNIVERSITY
GRADUATE SCHOOL
Thesis/Dissertation Acceptance

This is to certify that the thesis/dissertation prepared

By Joshua M. Goysich Nelson

~~Using~~ Using **PIEZOELECTRIC GENERATION TO HARVEST ENERGY FROM TURBULENT AIR FLOW**

For the degree of Master's of Science

Is approved by the final examining committee:

Mark French

Chair

Jeffrey J. Evans

William J. Hutzal

To the best of my knowledge and as understood by the student in the *Research Integrity and Copyright Disclaimer (Graduate School Form 20)*, this thesis/dissertation adheres to the provisions of Purdue University's "Policy on Integrity in Research" and the use of copyrighted material.

Approved by Major Professor(s): Mark French

Approved by: Gary Bertoline

Head of the Graduate Program

3/5/10

Date

**PURDUE UNIVERSITY
GRADUATE SCHOOL**

Research Integrity and Copyright Disclaimer

Title of Thesis/Dissertation:

USING PIEZOELECTRIC GENERATION TO HARVEST ENERGY FROM TURBULENT AIR
FLOW

For the degree of Master's of Science

I certify that in the preparation of this thesis, I have observed the provisions of *Purdue University Teaching, Research, and Outreach Policy on Research Misconduct (VIII.3.1)*, October 1, 2008.*

Further, I certify that this work is free of plagiarism and all materials appearing in this thesis/dissertation have been properly quoted and attributed.

I certify that all copyrighted material incorporated into this thesis/dissertation is in compliance with the United States' copyright law and that I have received written permission from the copyright owners for my use of their work, which is beyond the scope of the law. I agree to indemnify and save harmless Purdue University from any and all claims that may be asserted or that may arise from any copyright violation.

Joshua M. Goysich Nelson

Printed Name and Signature of Candidate

03-05-2010

Date (month/day/year)

*Located at http://www.purdue.edu/policies/pages/teach_res_outreach/viii_3_1.html

USING PIEZOELECTRIC GENERATION TO HARVEST ENERGY FROM
TURBULENT AIR FLOW

A Thesis

Submitted to the Faculty

of

Purdue University

by

Joshua M. Goysich Nelson

In Partial Fulfillment of the

Requirements for the Degree

of

Master of Science

May 2010

Purdue University

West Lafayette, Indiana

To my wife, Nicole, who has been an excellent example of grace and strength while allowing me to begin and complete this work.

And to my Savior, without whose grace I would not even exist.

ACKNOWLEDGMENTS

The author would like to thank Dr. R. Mark French, Dr. Jeffrey J. Evans, and Prof. William J. Hutzler for their guidance, the use of equipment and facilities, advice, and the encouragement to thoroughly understand.

TABLE OF CONTENTS

LIST OF TABLES	Page vi
LIST OF FIGURES.....	viii
GLOSSARY	ix
ABSTRACT	x
CHAPTER 1. INTRODUCTION	1
1.1. Objectives.....	1
1.2. Organization.....	1
1.3. Scope.....	2
1.4. Significance.....	2
1.5. Study Design.....	3
1.5.1. Hypotheses.....	4
1.5.2. Considerations.....	4
1.5.3. Variables and the Measurement Thereof.....	4
1.6. Assumptions, Limitations, and Delimitations.....	4
1.6.1. Assumptions.....	5
1.6.2. Limitations	5
1.6.3. Delimitations.....	5
CHAPTER 2. LITERATURE REVIEW	6
2.1. Past Studies.....	6
2.1.1. Applications of PEG	6
2.1.2. Physical PEG Optimization.....	8
2.1.3. PEG Circuit Optimization.....	9
2.2. Inferences.....	10
CHAPTER 3. THEORETICAL POTENTIAL.....	11
3.1. Analysis of Experiment.....	11
3.2. Maximum Power Available	11

	Page
3.3. Von Karman Vortex Shedding.....	14
3.4. Von Karman Application.....	15
CHAPTER 4. EXPERIMENTS.....	16
4.1. Explanation of Experiment	16
4.1.1. Test Rig.....	17
4.1.2. Initial Circuit Design.....	18
4.2. Bench Testing Procedure	19
4.3. Pre-Experimental Set-up and Measurements.....	20
4.4. Initial Test	23
4.5. Road Test	23
CHAPTER 5. RESULTS AND DISCUSSION.....	25
5.1. Initial Test Results	25
5.2. Road Test Results	31
5.2.1. System Noise	32
5.2.2. Piezoelectric OCV Characteristics.....	33
5.2.3. Piezoelectric CCV Characteristics	35
5.2.4. RMS Values	38
5.2.5. Voltage Frequency Characteristics	39
5.3. Series and Parallel Circuit Issues.....	42
5.4. Power Considerations	42
5.5. Effect on Drag.....	44
CHAPTER 6. CONCLUSION.....	45
BIBLIOGRAPHY	48
APPENDIX	51

LIST OF TABLES

Table	Page
Table 4.1. Wind tunnel velocities (given in m/s).....	21
Table 4.2. LCR measurements for piezoelectric elements	22
Table 5.1. OCV and calculated RMS, CCC, and power values.....	38
Appendix Table	
Table A-1. Maximum power data.....	51
Table A-2. Piezoelectric element efficiency	52

LIST OF FIGURES

Figure	Page
Figure 3.1. Drag force as a function of velocity ($C_D = 0.34$, $A = 0.1479 \text{ m}^2$)	12
Figure 3.2. Maximum power available at various velocities	13
Figure 4.1. Assembled wind tunnel	16
Figure 4.2. Various PEG design ideas	18
Figure 4.3. Charge pump circuitry	19
Figure 4.4. Square nozzle.....	20
Figure 4.5. Round nozzle	21
Figure 4.6. Piezoelectric circuit representation.....	22
Figure 4.7. Road test piezoelectric element mounting.....	23
Figure 5.1. OCV for a single piezoelectric at 15 m/s	25
Figure 5.2. CCV for a single piezoelectric at 15 m/s across a 1 k Ω resistor.....	26
Figure 5.3. OCV for two series piezoelectric elements at 15 m/s	26
Figure 5.4. CCV for two series piezoelectric elements at 15 m/s across a 1 k Ω resistor	27
Figure 5.5. OCV for two parallel piezoelectric elements at 15 m/s.....	27
Figure 5.6. CCV for two parallel piezoelectric elements at 15 m/s across a 1 k Ω resistor.....	28
Figure 5.7. Instantaneous power from a single piezoelectric element using LabVIEW	29
Figure 5.8. Instantaneous power from two series piezoelectric elements using LabVIEW	30
Figure 5.9. Instantaneous power from two parallel piezoelectric elements using LabVIEW	30
Figure 5.10. Sample velocity vs. time for road test	31
Figure 5.11. Welch power spectral density estimate for OCV from one element at 0 m/s	32

Figure	Page
Figure 5.12. OCV vs. velocity for a single piezoelectric element	33
Figure 5.13. OCV vs. velocity for two piezoelectric elements in series	34
Figure 5.14. OCV vs. velocity for two piezoelectric elements in parallel	35
Figure 5.15. CCV vs. velocity for a single piezoelectric element	36
Figure 5.16. CCV vs. velocity for two piezoelectric elements in series	37
Figure 5.17. CCV vs. velocity for two piezoelectric elements in parallel	38
Figure 5.18. Welch power spectral density estimate for a single element.....	39
Figure 5.19. Welch power spectral density estimate for two elements in series	40
Figure 5.20. Welch power spectral density estimate for two elements in parallel	41

GLOSSARY

- MEMS - Micro Electromechanical System
- OCV – Open-circuit voltage
- PEG - Piezoelectric Generator or Piezoelectric Generation- A device that utilizes the piezoelectric effect to the end of creating electricity to be used by another device or the application of said device
- Piezoelectric – A material that exhibits the property of creating a voltage when stressed (Sodano, Inman, & Park, 2005)
- CCC – Closed-circuit current (through a 1 k Ω resistor)
- CCV – Closed-circuit voltage (across a 1 k Ω resistor)

ABSTRACT

Nelson, Joshua M. G. M.S., Purdue University, May, 2010. Using Piezoelectric Generation to Harvest Energy from Turbulent Air Flow. Major Professor: Dr. R. Mark French

The tasks of generating, harvesting, and converting energy have long been ones crucial to the human race. As such, environmental concerns, population increase, personal energy consumption, and diminishing resources have led to a focus on new methods and possibilities. A set of factors has influenced this research, among which was a desire to steward resources better, the inefficiencies of many current generation technologies, and the rising cost of fuel.

Although piezoelectric generation (PEG) has been researched and used to power small devices, this generation technique is undeveloped, especially on a large scale. This research focuses on the conversion of air turbulence to electrical energy via a piezoelectric generator.

After a literature review was conducted, calculations were performed to determine energy potential. Bench tests were performed to determine the characteristics of the material. Road tests were then carried out utilizing a thin-film piezoelectric material. Data such as air velocity and voltage were collected. It was found that the piezoelectric effect can be used to harvest energy from turbulent air flow. However, with the method and material used, this is not an efficient means of energy harvesting; power generated was less than 1 microwatt.

CHAPTER 1. INTRODUCTION

This chapter defines the purpose of the study and sets out its objectives. Layout of this thesis, possible hypotheses, and other considerations are also discussed.

1.1. Objectives

This research was designed to investigate whether piezoelectric elements could be used on a moving body (such as an automobile) to harvest and convert wind energy. Presumably, this energy could then be used to power some device onboard the body, but this study was limited to exploring the concept of such harvesting. This experiment was performed in a wind tunnel in order to establish a controlled environment and then carried out in detail in a series of road tests.

Specific objectives included:

1. Determine theoretical power potential
2. Quantify amount of power experimentally observed
3. Observe power density and efficiency

1.2. Organization

This thesis contains six chapters. This first introduces the topic of piezoelectric generation and the scope of the project. The second chapter looks at relevant literature and applies it to the topic at hand. The third analyzes the experiment from a mathematical perspective and the experiment itself is discussed in the fourth chapter. Results and discussions follow in the fifth chapter, while the final chapter concludes the study.

1.3. Scope

The intent of this project was to research, measure, and document the amount of power that can be harvested through the use of a piezoelectric sheet on a moving vehicle actuated by turbulent airflow. Although many materials are available, sheets of polyvinylidene fluoride (PVDF) were used. PVDF is relatively low in cost and can be made in a variety of physical sizes. As harnessing wind energy was the focus, a sheet-type piezoelectric element was selected. This format offers a high surface-to-volume ratio, and thus can be moved by air easily.

It was not practical at this point, nor was it the focus of this research to determine the most efficient placement of the piezoelectric collector, only to determine the possibilities. It is likely that efficiency will be higher at some spots than others; this, however, will be left to future work.

Optimum circuit designs was also not covered. Other researchers have studied this topic (Ottoman & Lesieutre (2003), Han, et al (2004)), and have begun to optimize the power conditioning circuitry for PEG.

Although material strength and durability are general concerns, they were not dealt with at this point.

As power generated greatly depends on air velocity, various velocities were taken into account.

1.4. Significance

New power generation techniques are of great value. As population increases, so do its energy demands, if simply because of numbers. Current technologies such as coal and petroleum engines are not indefinitely sustainable. Thus, it is profitable to research new methods of producing energy that have the ability to replace or at least alleviate reliance on these limited forms.

Research regarding macro piezoelectric generation (PEG) is largely absent. According to Kim (2002), PEG is a largely un-researched topic. Many piezoelectric materials are able to output a large amount of voltage, but a relatively small amount of

current. Because of this characteristic and others, PEG has only recently been considered as a power source.

However, PEG offers many advantages. First, it is a solid-state technology. These devices can be compact and durable. This is an advantage over other generation technologies, as it leads to a more robust device that may also have lower manufacturing costs. Second, this application of PEG focuses on utilizing energy that is usually ignored, such as vibrations or turbulent airflow. These sources of energy are usually dissipated as heat. This may be thought of as ‘free’ energy within a closed system. Third, although PEG offers low current, the voltage potential and efficiency are notable. Recent studies have shown piezoelectric efficiency to be as high as 70%.

Batteries are another reason to consider PEG. In installations that are difficult to reach or explore a battery that needs to be replaced is a complicating factor. Many new types of batteries, while technologically advanced, are also constrained by cost, size, or weight. In addition, every PEG replacement power cell could mean one less battery needing disposal at the end of its comparatively short life.

Perhaps the strongest reason to pursue PEG lies with the type of energy it utilizes. Vibrations are present in many bodies, such as humans, buildings, and vehicles. Many times these vibrations are ignored or even dissipated, as is the case with shock absorbers. Whether it be a wristwatch or a transmitter on a tower PEG offers the possibility of converting this untapped source.

Current piezoelectric technology and materials would not allow one to replace all batteries or other power sources. Although characteristic piezoelectric voltage output is high, the current is quite low. As technology progresses and new materials are found or formulated, however, PEG may be able to replace conventional generation systems. This may even be possible on a device as complicated as a vehicle.

1.5. Study Design

A quasi-experimental study was used to determine how much power could be harvested from airflow using a piezoelectric sheet mounted inside a wind tunnel and on a vehicle. The exploratory nature of this study and the small sample size made statistical

inference less practical. Therefore, the quasi-experimental study method was chosen. The quasi-experimental study is described by Sekaran (2002). In a study of this type, null and alternative hypotheses are set, but the hypothesis is selected at the end based not on statistical analysis, but on what the individual results of the study show.

1.5.1. Hypotheses

Null and alternative hypotheses were established, as shown below.

H0: No useable power can be harvested from this setup

Ha: Useable power can be harvested from this setup

1.5.2. Considerations

One problem with this approach is the definition of “usable power.” Certain devices require little power, while others require much. As one of the intended final applications of this research is to power on-board vehicle electronics (specifically LED lights), “usable power” is defined here as enough power to activate a single, low-power LED (around 20 mW).

1.5.3. Variables and the Measurement Thereof

The dependant variable was air velocity. The independent variable was voltage.

In order to measure the variables, a National Instruments USB-6215 data acquisition system, an OROS OR24 data acquisition system, and a Tecktronix TDS 380 oscilloscope were used (NI DAQ, OROS DAQ, and scope hereafter, respectively). Measurements included volts from the PEG, and voltage from the anemometer (later converted to m/s—see Chapter 4).

1.6. Assumptions, Limitations, Delimitations

This section further focuses the study by stating assumptions, limitations, and delimitations.

1.6.1. Assumptions

- Piezoelectric element representative of all materials
- Resistance from wires was negligible
- Interference from ambient sources was negligible
- Test velocities were a representative sample (approximately 0 m/s – 22 m/s)
- Air velocity was only in one direction
- Air density was constant at 1.233 kg/m³
- Air dynamic viscosity was constant at 1.807×10^{-5} kg/(m*s)

1.6.2. Limitations

- Since wind and airflow are chaotic, destructive interference may have been present
- Cross-sectional area of wind tunnel fixed
- Maximum wind tunnel air velocity approximately 16 m/s
- Maximum anemometer velocity approximately 22 m/s

1.6.3. Delimitations

- Difference in piezoelectric materials and their generation capabilities were not covered
- Optimum piezoelectric placement was not covered
- Effect on aerodynamic drag was not measured
- Durability was not a factor in this study
- Various PEG circuitry and optimization techniques thereof were not covered
- Optimum poling was not discussed
- Optimum piezoelectric electrode placement was not covered

CHAPTER 2. LITERATURE REVIEW

In order to develop a solid foundation from which to build this study, a literature review has been conducted. This review is presented below, focused on three main topics: Applications of PEG, Physical PEG Optimization, and PEG Circuit Optimization.

2.1. Past Studies

A piezoelectric material is one that creates voltage when force is applied to it and vice-versa. This effect was discovered by Pierre and Jacques Curie in 1880.

Piezoelectric materials are both man-made and naturally occurring. Much research has been done on the topic of piezoelectric devices as actuators (those devices that send vibrations or signals) and receivers (devices that receive vibrations or signals).

2.1.1. Applications of PEG

Research surrounding piezoelectrics is numerous. However, piezoelectric generation is a fairly recent concept. Some of the earliest research found dealt with powering portable computers via human movement (Starner (1996)). Starner investigated various activities (such as breathing and walking), quantified the amount of energy available, looked at various harvesting technologies, and suggested whether or not it was practical to harvest energy from this activity. It was found that walking seemed to be the best method for harvesting energy and that two technologies provided a way to harvest this energy: piezoelectric and magneto electric generation (Starner (1996)).

Small-scale harvesting from human activity is a concept that others have investigated as well. Using a piezoelectric transducer, Ramsey and Clark collected energy from blood pressure fluctuations (2001). Using a circular thin-plate transducer and a piezoelectric element with a 31- poling direction, they were able to obtain 2.5 μW .

While this was well below their goal of 10 μW , they did show that ample power was available from the source (blood pressure). In addition, mathematical analysis seems to indicate that given a cyclical changing force, power output is exponentially related to area of the sensor and also exponentially related to thickness. However, as the force and fluctuations were relatively small (1Hz cyclic pressure of 5333 N/m^2), these results may not be generalizable to larger applications.

Numerous studies have been performed regarding power harvesting for MEMS and wireless sensor networks. Roundy and Wright (2004) used a PEG of less than 1 cm^3 to power a wireless transmitter, although only with a 1.6% duty cycle. Song, et al (2007) found that the impedance of the PEG was lowered with multiple layers and hypothesized that a PEG of this type could power a sensor without additional electronics.

It is not only power generation for MEMS that benefits from the use of piezoelectric materials. Dong, et al (2004) built a piezoelectric transformer with an out-to-in voltage ratio higher than that of some electromagnetic transformers (the more conventional design). These studies and others point to the possibility of high piezoelectric efficiency, which is imperative to energy conversion and generation.

Ogando (2007) researched various uses of active vibration control technology, sometimes labeled "adaptronics." Although the field of adaptronics includes more than piezoelectrics, they play an important role. Ogando states, "As part of a vibration control system, these actuators can be designed to address a wide range of frequencies--from 50 to 1,000 Hz--depending on the application needs." The characteristics of piezoelectric devices enable them to operate over a large range.

The practicality of piezoelectric devices varies widely from inexpensive sensors to costly actuators. Grove & Ehle (2002) developed a simple device that could measure force and energy utilizing the voltage output from a piezoelectric cell in order to demonstrate the difference between the two to physics classes. This device could be built by a layperson at a low cost. In contrast, Friedman, et al (2007) used an array of piezoelectric actuators and receivers to counteract vibrations in textile machinery. Although comparatively expensive at the time of this writing, such technology may prove useful, as increased output may outweigh implementation. In addition, the vibrations

produced by this system were substantial; enough to reduce machine vibration by as much as 80% using large voltage. Given this, in an environment where many vibrations are present (such as on a moving vehicle), it may be possible to generate a large voltage.

2.1.2. Physical PEG Optimization

Smith, et al (1984) showed that small, cylindrical piezoelectric cells embedded in a matrix can act as a single unit. This may provide the possibility of creating a low-cost piezoelectric paint, although this theory is yet untested.

Piezoelectric device efficiency is a topic mentioned by Friedmann, et al (2007), Kim, et al (2005), and Dong, et al (2006). Friedmann, et al showed that simply by changing the location of a piezoelectric actuator, vibrations could be reduced by as much as 80%. This reduction in vibration could be related to energy available for harvesting. Kim, et al calculated that the amount of energy output by the PEG is directly related to the ratio of substrate thickness to piezoelectric thickness. Dong, et al, in studying a former design, found that the magnetoelectric/piezoelectric transformer had a higher voltage gain and larger bandwidth than current data. These data show that piezoelectric generation can be an efficient mode of generation.

Tantamount to device efficiency is material efficiency. Funasaka, et al (1998) studied PEG in two devices, one using lead zirconate titanate (PZT), the other lithium niobate (LiNbO_3). LiNbO_3 was found to have higher conversion efficiency than PZT, which is the conventional material. In cases such as the one at hand, materials may be developed, discovered, or utilized because they provide specific characteristics, such as durability, manufacturability, and power generation efficiency.

Kim (2002) studied another area of PEG efficiency: electrode placement. Three devices were tested, each of the same material and dimensions. Two underwent a repoling and reapplying of electrodes; the third remained unchanged. The repoling method used here is named the interdigitated method. In this method, one begins with a piezoelectric element that has the poling direction perpendicular to its surface. The electrodes are removed or created in such a fashion that they resemble the teeth of a comb. Next high voltage is applied to the electrodes while the temperature is held above

the Curie temperature. The electric field changes the poling direction and after cooling down, the piezoelectric element has approximately the same poling direction. In addition to repoling, the electrodes were placed in accord with calculated optimum placement. All three were placed in a test apparatus with their edges fixed and subject to a changing air pressure on one side. Data about air pressure and voltage were collected via separate boards and computers and then graphed and analyzed. Regrouping and repoling of the PEG in the 33 direction (interdigitated method) produces more efficiency, as did the change in electrode placement.

Frequency of driving vibrations is another factor in PEG efficiency (Poulin, et al (2003)). As a basic rule, the closer the driving vibrations are to the natural frequency of the device, the more efficient it will be. Lu, et al (2002), however, showed that some devices will increase in output as frequency increases. But even to this suggestion there is a limit, as their research also shows that above a certain point, efficiency actually decreases.

2.1.3. PEG Circuit Optimization

In addition to optimizing the physical design of the PEG, the power conditioning circuitry can also be improved. As the physical design of this experiment is different than that of one for MEMS, circuit design is more relevant to this study.

One of the many interesting studies determined that the energy generated by a piezoelectric device subject to random vibrations could be stored via a battery or capacitor for later use (Sodano, et al (2005)). Other investigation shows that circuits with very high efficiencies can be designed for PEG. Han, et al (2004) used a charge pump, composed of a bank of capacitors and switches, to increase the efficiency of a PEG circuit. Efficiencies of this new circuit were as much as 92% higher than previous designs, leaving more power available for use outside of the PEG.

Of interesting note is the research cited by and expounded on by Makiyara, et al (2006). Because of the power generating capabilities of piezoelectric devices, they can be used not only to control vibrations, but to power themselves while doing so. Guyomar, et al (2000) showed a similar concept. In their research, a device was designed

that used a piezoelectric element and circuit to provide mechanical damping while powering itself. Three designs were studied: a piezoelectric element with an open circuit, a piezoelectric element with a switch on a short circuit, and a piezoelectric element with a switch on an inductor. Whereas the first two designs had a narrow frequency within which their damping was most effective, the damping of the switched inductor circuit had a wider effective range. From this, one may note that this design harvested more energy from the mechanical system. Although PEG was not the focus of this research, the same design could be used for generation.

Priya (2007) conducted a survey of various advances in PEG. Various studies were cited, yielding gains in efficiency from adding multiple layers, increasing mass (for cantilever-type PEG), and increasing damping. Novel ideas were also discussed, such as using an “eel” design for hydroelectric PEG and a wind turbine that generated electricity using piezoelectric elements.

2.2. Inferences

The background information seems to point to PEG as a possible replacement power source for batteries on a small scale. As size of the piezoelectric element can be related to the power output of the PEG, this technology may be scalable for use in larger applications. Because it utilizes dissipated energy, PEG could greatly improve efficiency and decrease waste in many applications. High-energy conversion efficiencies (greater than 90%) are possible given the optimum circuit and overall PEG design. It is the hope of the author that these theories could be applied to transportation in such a way that would alleviate current fuel consumption and avail itself of use on the next generation of vehicles or as a retrofit on current ones.

CHAPTER 3. THEORETICAL POTENTIAL

In order to build validity, a mathematical analysis of the maximum power available from the flow has been conducted.

3.1. Analysis of Experiment

Because of the pioneer nature of this application, a mathematical analysis is worthwhile in not only the design of the experiment, but the conclusions drawn from it. Maximum power available from the turbulent flow aided determining the feasibility of this research. Material efficiency was also taken into consideration.

3.2. Maximum Power Available

Figure 3.1 below shows the calculated relationship between velocity and aerodynamic drag force available using the formula for drag force:

$$F = C_D * A * (\rho * v^2) / 2. \quad (\text{Eq. 3.1})$$

Here, F is the force of the aerodynamic drag, C_D is the dimensionless drag coefficient, A is the cross-sectional area of the body in question, ρ is the density of the fluid (in this case air), and v is air velocity.

The frontal swept area of the vehicle used (1993 Acura Legend) was 0.1479 m^2 . The drag coefficient for this vehicle was $C_D = 0.34$.

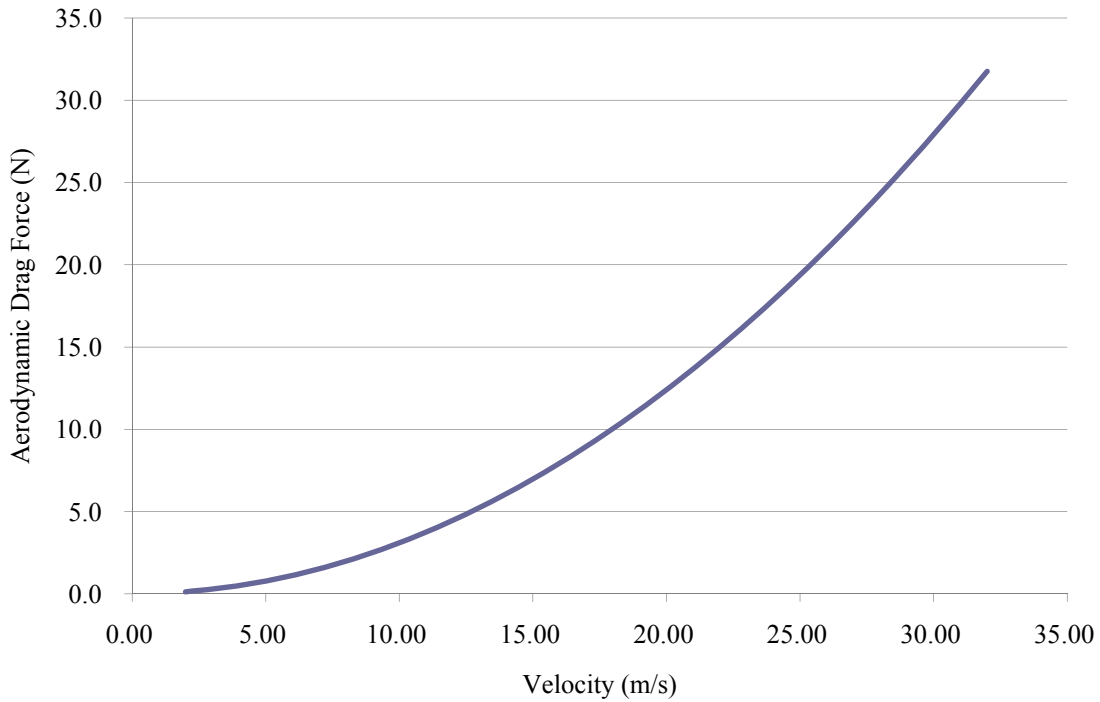


Figure 3.1. Drag force as a function of velocity ($C_D = 0.34$, $A = 0.1479 \text{ m}^2$).

Of the total drag on a vehicle, 70% can be said to occur at the front of the vehicle, 10% occurs along the sides and top, and 20% occurs at the rear; of this drag along the sides and rear, turbulence only accounts for half (Gillespie (1992)). Using these guidelines, it is possible to determine the maximum force present along the top of the moving body:

$$F_{\text{TOP}} = F * 0.50 * 0.10. \quad (\text{Eq. 3.2})$$

Power can then be found by multiplying this drag force by the air velocity, as the air velocity acting on the piezoelectric element cannot be greater than the air velocity acting on the object:

$$P_{\text{MAX}} = F_{\text{TOP}} * v. \quad (\text{Eq. 3.3})$$

Figure 3.2 shows maximum power available along the top of the body as a function of wind velocity. The data for this figure may be found in Table A-1 in the Appendix. The star at 30 m/s represents highway speeds (approximately 65 mph).

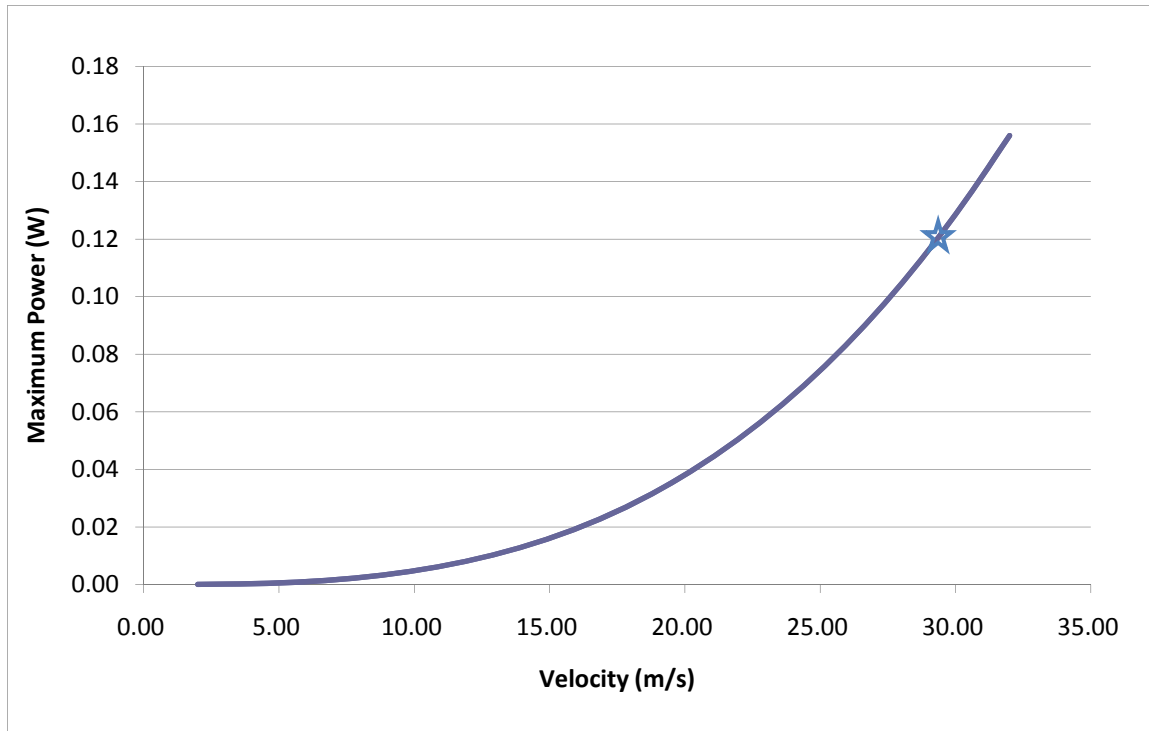


Figure 3.2. Maximum power available at various velocities.

The goal is to remove power from the flow of air over the body, but it is not possible to harvest all of the available power. As area and density were assumed to be constant, velocity and the drag coefficient were the only things that could be changed. Figure 3.2 shows how power available varies with velocity. Adding a PEG of the type mentioned here will change the drag coefficient in some way. Whether this will increase or decrease the drag coefficient is unknown at this time, and was not tested in this study.

There is at least one more factor to consider here. The exact nature of turbulent flow is an ongoing problem in the fields of engineering and physics. Each turbulent situation seems to be unique, with its own characteristics. No singular solution has been derived. As such, it is difficult to determine exactly how much of the power in the turbulent flow could be harvested. Although the PEG discussed here is not of the wind-turbine type, the Betz limit can still be used as a benchmark for wind generation. The Betz limit states that the maximum amount of power that can be extracted from an airstream is 59.3%. This results of this calculation are shown in Table A-1.

The final factor to consider here is the mechanical-to-electrical conversion efficiency of the piezoelectric material. According to manufacturer data, PVDF has a maximum mechanical-to-electrical efficiency, k_{33} , of 12%. The 33 subscript here indicates that the force applied passes through the surface of the electrodes on the piezoelectric element. Much higher conversion efficiencies (70% and higher) are available with rigid, crystal-type piezoelectric materials, such as PZT. However, these do not lend themselves well to the application used in this study. Therefore, the maximum power possible from this material in this situation is given by:

$$P_{\text{PEG}} = P_{\text{MAX}} * k_{33}. \quad (\text{Eq. 3.3})$$

This calculation is reflected in the last column of Table A-1. Thus, the maximum power at the speeds tested in this study (22 m/s) is 0.0507 W (507 mW). Based on the hypotheses discussed in section 1.5, there is enough power available.

3.3. Von Karman Vortex Shedding

As turbulent flow is chaotic in nature, many frequencies are present. However, as the most power may be obtained at the resonant frequency, it is beneficial to excite the piezoelectric element at this resonant frequency. One way to do this is to induce von Karman vortex shedding using a cylinder. Von Karman vortex shedding is a phenomenon in which vortices are produced on either side of a cylinder placed inside a free-flow stream. These vortices are produced in an alternating fashion at a specific frequency that is dependent upon the stream velocity and the diameter of the cylinder, among other things.

The diameter of a cylinder needed to produce vortex shedding of a certain frequency is given by:

$$d = \{ 0.198 * [1 - (19.7 / \text{Re})] * v \} / f, \quad (\text{Eq. 3.4})$$

where d is the diameter of the cylinder in meters, Re is the Reynolds number, v is the flow velocity in meters per second, and f is the frequency in hertz. Given that:

$$\text{Re} = (v * d * \rho) / \mu, \quad (\text{Eq. 3.5})$$

Equation 3.4 then becomes:

$$d = (0.198 * v) / [f + (3.9006 * \mu) / \rho]. \quad (\text{Eq. 3.6})$$

3.4. Von Karman Application

The original intent was to use this information inside the wind tunnel. However, after performing calculations and inspecting the wind tunnel, the idea was dismissed; the area of the wind tunnel was so small that a cylinder would have taken up the bulk of the tunnel, serving not produce the desired effect, but only to disrupt the flow of air. A larger wind tunnel would have alleviated this issue. A smaller cylinder could also have been used had higher velocities been available.

CHAPTER 4. EXPERIMENTS

In this chapter, the physical experiments are presented. Both the bench test and the road test are explained in detail.

4.1. Explanation of Experiment

As this study is of an experimental nature, bench testing was chosen as the initial experiment. A 0.56 m long wind tunnel with a cross-sectional area of 0.0232 m^2 was employed to this end (see Figure 4.1). The wind tunnel was measured to produce wind at a maximum air velocity of approximately 16 m/s.

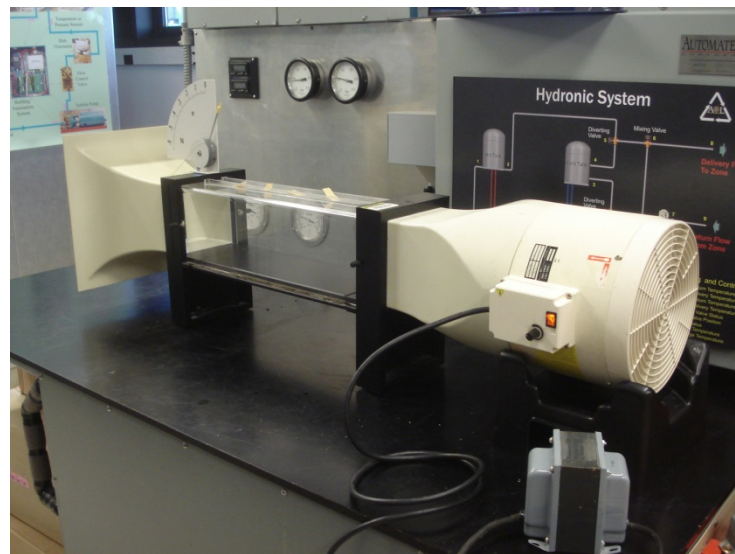


Figure 4.1. Assembled wind tunnel.

Air velocity was measured using a hot-wire anemometer which sent a 0-5 VDC signal to the NI DAQ; the software then converted this voltage signal to an air velocity measurement in meters per second.

The thin-film piezoelectric element was placed inside the wind tunnel such that airflow caused it to oscillate. The piezoelectric element was connected to the NI DAQ (see Section 4.1.1 for details). Open-circuit voltage (OCV) and closed-circuit voltage (CCV) (through a 1 k Ω resistor) from the piezoelectric element were measured using the NI DAQ. CCV was later converted to closed-circuit current (CCC). Power was then calculated using these measurements.

For the road test portion of the experiment, the same piezoelectric element configurations and anemometer were used. These components were mounted on a moving vehicle. The OROS DAQ and a laptop computer were used to collect voltage data from the piezoelectric element and the anemometer.

4.1.1. Test Rig

One of the benefits of the piezoelectric collector is its simplicity. This rig is made of a few simple elements: a piezoelectric sheet collector laminated to increase durability, the anemometer, and the measurement device (a DAQ or the scope).

The piezoelectric element is made of a thin layer of polyvinylidene fluoride (PVDF) mounted to a thin thermoplastic laminate. Various thicknesses were available, such as 52 μm and 27 μm . The 27 μm thickness was chosen in order to make the most use of the relatively low air velocities. In higher speed applications thicker piezoelectric elements could be used.

The collector was mounted to a vertical rod within the wind tunnel. Various arrangements were considered (Figure 4.2), but a flag-type element was chosen in order to maximize movement of the piezoelectric element. In contrast, the skin-type element may not be as efficient because of boundary-layer concerns. Close to a moving body, lower flow is present; ergo less energy would be available for harvesting.

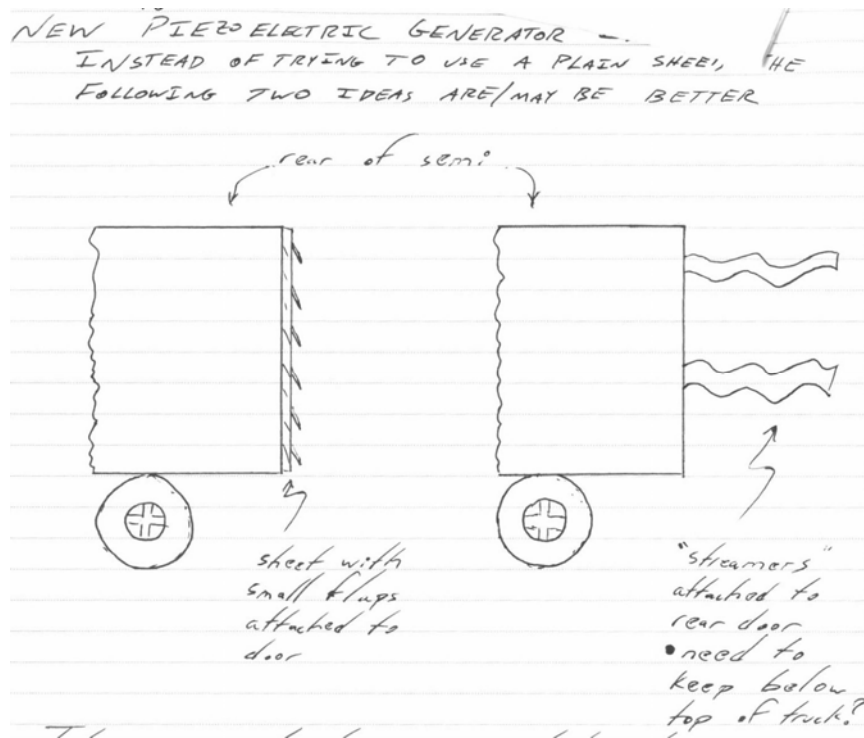


Figure 4.2. Various PEG design ideas.

4.1.2. Initial Circuit Design

As mentioned in Chapter 2, the charge pump is one of the most efficient PEG circuit designs. This circuit was adapted for this study; the diagram for this charge pump is shown in Figure 4.3. In this design, the piezoelectric element charges all four capacitors in parallel. The switches are then manually switched and the capacitors can be used in a parallel-series combination to power the LED. Note that here the piezoelectric element is represented by an AC voltage source.

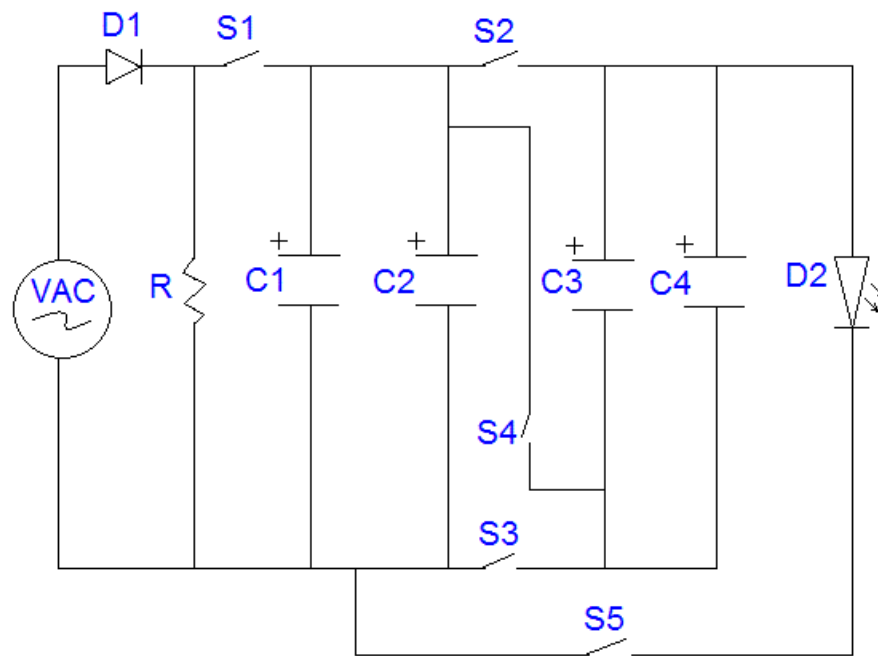


Figure 4.3. Charge pump circuitry.

This circuitry is operated manually as follows. First, the piezoelectric element is used to charge the four capacitors (C1-C4) in parallel by closing switches S1, S2, and S3. Once charged to maximum piezoelectric voltage, these switches are then opened. Next, switches S4 and S5 are closed. This allows capacitors C1 and C2 to be arranged in parallel; capacitors C3 and C4 are likewise arranged in parallel. These two parallel sets are then arranged in series. The capacitors then light the LED (D2).

After measuring the output of the piezoelectric element with the scope, it was found that the piezoelectric element did not produce enough voltage to switch the diodes. Therefore, this design was abandoned in favor of the piezoelectric element by itself.

4.2. Bench Testing Procedure

Using LabVIEW software, a program was created to measure OCV and CCV coming from the piezoelectric element as well as voltage from the anemometer. The signal range of the NI DAQ was ± 10 V with a resolution of 16 bits. After reading the

values, the software displayed all values graphically. The user could choose for the program to output the measurements to a text file. The data was checked against the scope to ensure accuracy.

4.3. Pre-Experimental Set-up and Measurements

In order to gather accurate data about each trial, pre-experiment readings were taken. Air velocity within the wind tunnel was first measured. Two nozzle options were available: a square nozzle and a smaller, round one (Figures 4.4 and 4.5). Velocities were taken from a nine-point grid pattern inside the tunnel and are reported in Table 4.1. In this table, rows and columns are labeled with physical locations (top, middle, etc). These locations graphically represent the points measured within the tunnel.

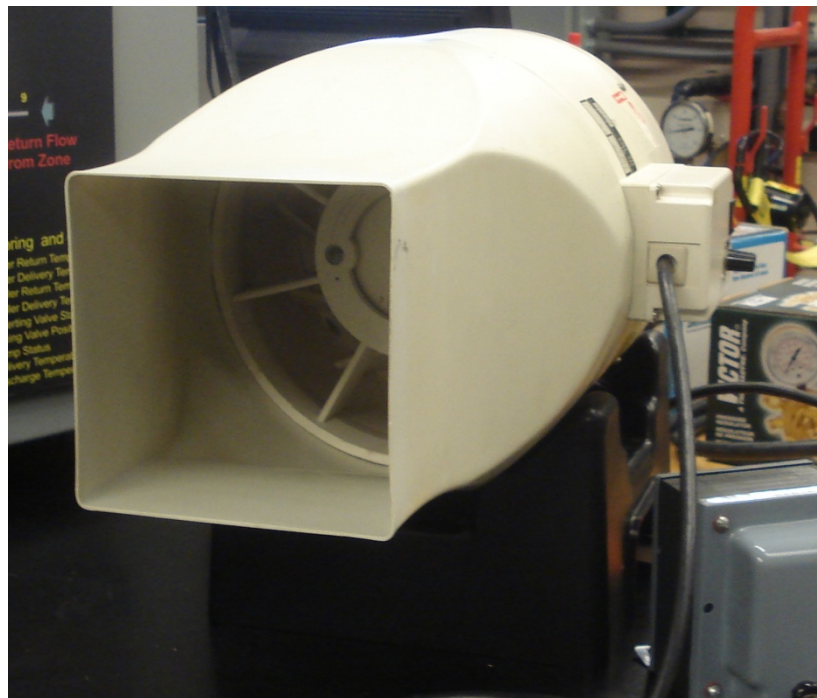


Figure 4.4. Square nozzle.

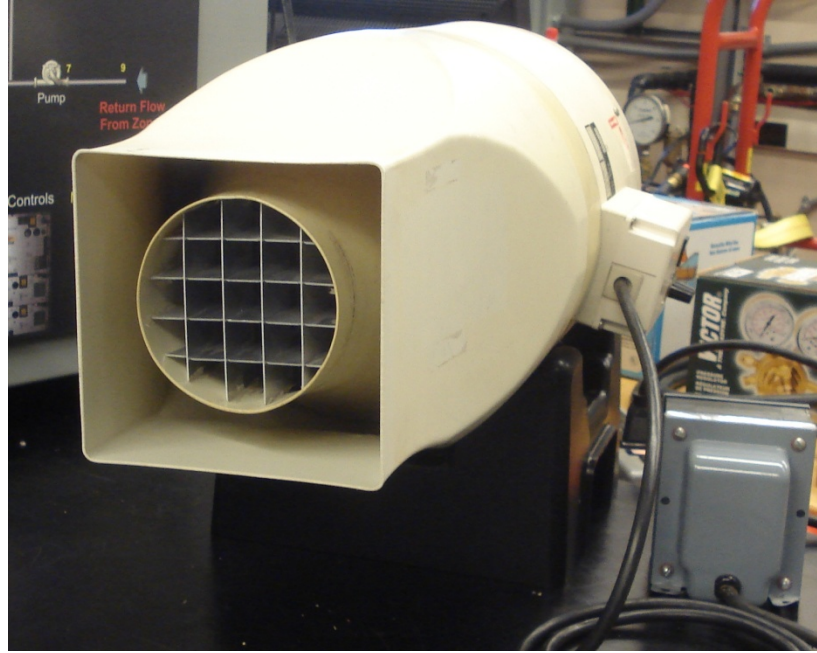


Figure 4.5. Round nozzle.

Table 4.1. Wind tunnel maximum velocities (given in m/s).

	Square Nozzle				Circular Nozzle		
	Left	Center	Right		Left	Center	Right
Top	7.92	8.94	8.03	Top	3.35	11.79	2.31
Middle	11.68	9.04	9.04	Middle	5.89	13.21	2.54
Bottom	8.84	10.26	8.74	Bottom	2.74	5.59	1.47

From Table 4.1 it can be seen that the smaller, round nozzle provided the highest wind velocity (13 m/s—approximately 30 mph). Although this velocity is more concentrated, the profile of the piezoelectric element fits well within the diameter of the nozzle.

An LCR meter (Protek LCR Meter Z8200) was used to measure the capacitance and AC resistance of the piezoelectric element at 1 kHz. All six piezoelectric elements were measured in order to obtain accurate results. The results are displayed in Table 4.2. Note the capacitive nature of the piezoelectric material.

Table 4.2. *LCR measurements for piezoelectric elements.*

	X_C (k Ω ; at 1kHz)	C (nF)	R (Ω)
1	7.643	20.82	120
2	7.600	20.95	116
3	7.593	20.97	114
4	7.554	21.06	117
5	7.523	21.15	116
6	7.600	21.30	131
Averages	7.586	21.04	119

These values can be of use when looking at the circuit representation of a piezoelectric element. This is shown In figure 4.6. Note that the piezoelectric element is represented by an AC voltage source, a capacitor, and a resistor in series. This representation is consistent with the literature (e.g. Priya (2007)). The values for RPEG and CPEG are those shown in Table 4.2. For the OCV measurements, the circuit was connected directly to the DAQ at points 1 and 2. For the CCV measurements, a 1 k Ω resistor was also attached at points 1 and 2, in parallel with the piezoelectric element.

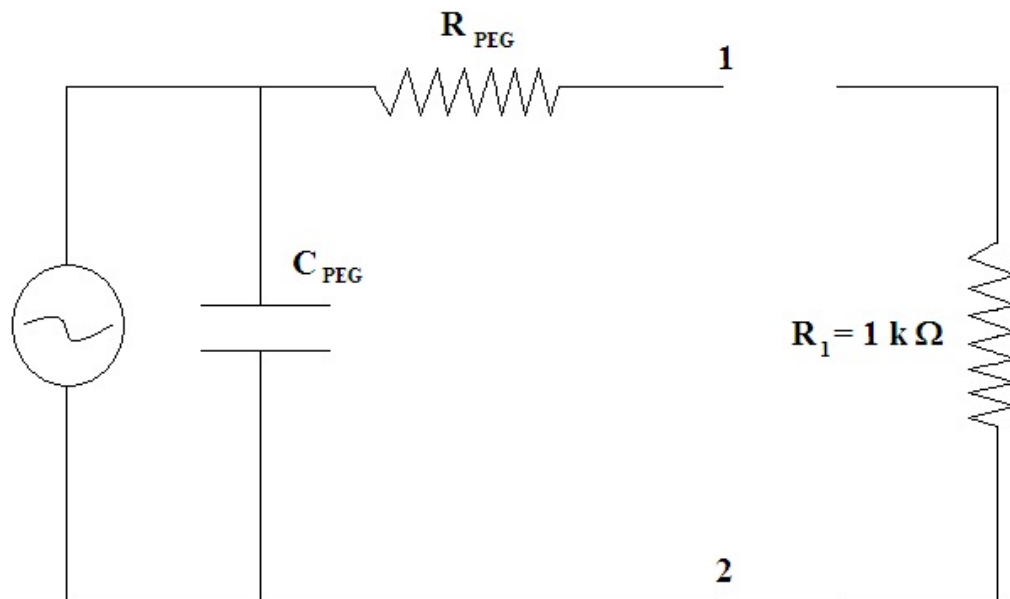


Figure 4.6. Piezoelectric circuit representation.

4.4. Initial Test

For the initial test, OCV and CCV were obtained at various air velocities using the scope. The test was then repeated using the LabVIEW software. CCC was found by measuring the voltage across a 1 k Ω resistor. The test was performed with a single piezoelectric element, two elements in series, and two elements in parallel. The results for this test can be found in section 5.1.

4.5. Road Test

For the road test, the piezoelectric element was mounted to the top of a moving vehicle (see Figure 4.7). This placement simulated the placement in the wind tunnel—one with little interference from other objects. Once again, OCV and CCV were measured for three different scenarios: a single piezoelectric element, two elements in series, and two elements in parallel. The same anemometer was used for the road test. CCV was converted to CCC after the data was collected.

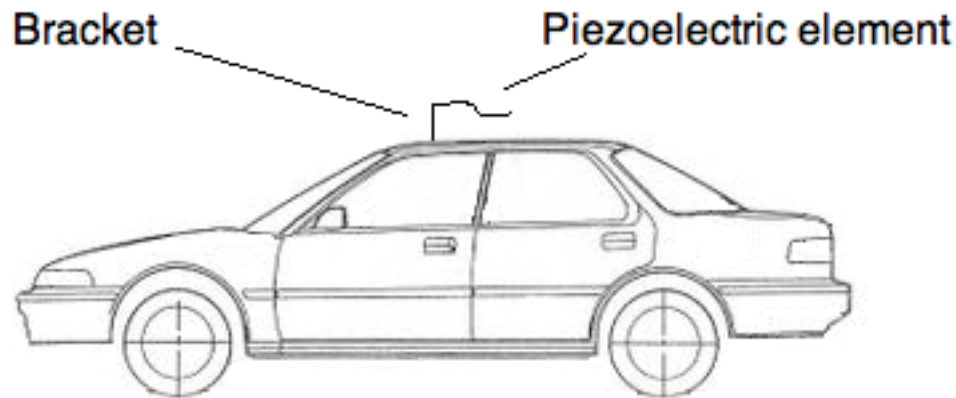


Figure 4.7. Road test piezoelectric element mounting.

The OROS DAQ was utilized for the road test. This allowed for simpler measurements than the NI DAQ and reduced the computing requirements.

For each of the six tests (OCV and CCV for each of the following: the single element, two elements in series, and two elements in parallel), the vehicle was brought to

above 22 m/s and then measurements were taken. The vehicle was then brought to a stop during the 30 second test, thereby reducing the air velocity.

In addition to obtaining the Root-mean-square (RMS) values for each of these tests, the OROS DAQ allowed the frequency content of the piezoelectric output to be observed.

CHAPTER 5. RESULTS AND DISCUSSION

Results of each test and inferences from them are discussed in this chapter.

5.1. Initial Test Results

In the initial test, OCV and CCC values were obtained. Figures 5.1 – 5.6 show scope screen shots at the maximum air velocity tested (15 m/s—approximately 34 mph). It should be noted that this setup had an RMS noise of 0.002 V and a PP noise of 0.014 V with the air velocity at 0 m/s, rendering any readings at or below these values unusable. This could be due to a number of factors, including movement of people within the room and the HVAC system. Although the wind tunnel was an enclosed space, a vent for the HVAC system was located directly above the bench. A piezoelectric is a very sensitive device and can pick up pressure variations as small as those mentioned here. This effect is most evident in the CCV figures.

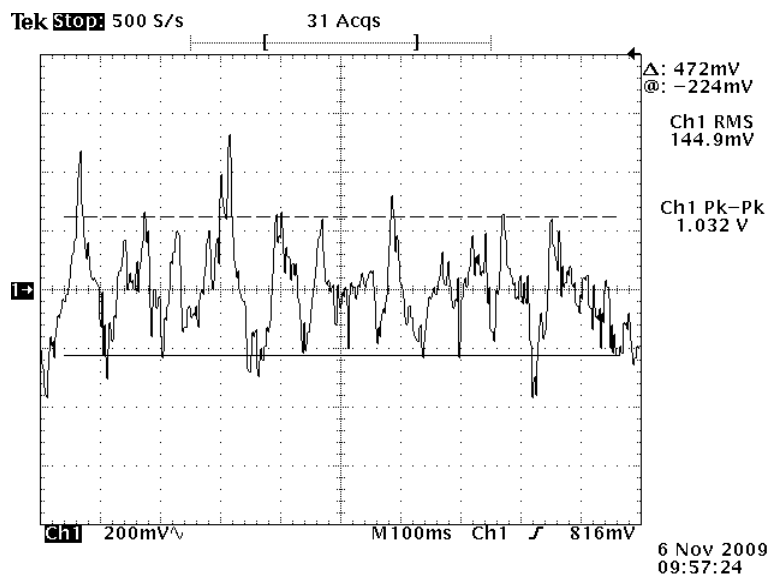


Figure 5.1. OCV for a single piezoelectric at 15 m/s.

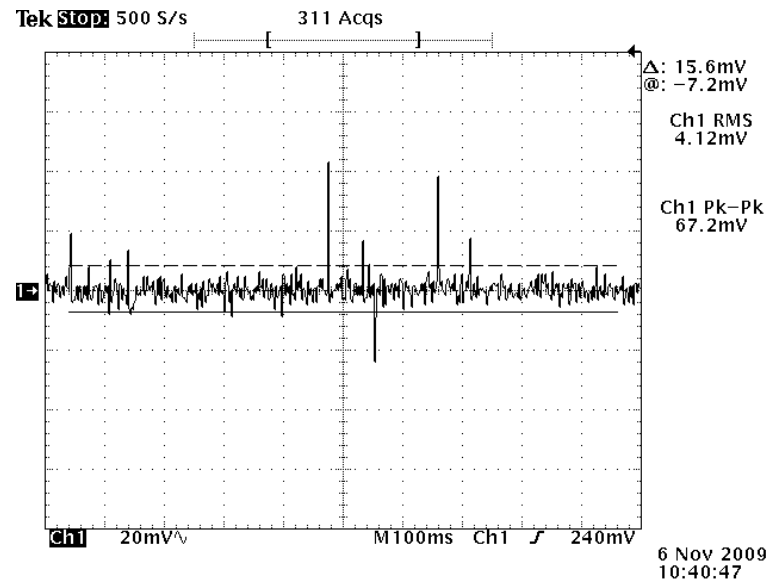


Figure 5.2. CCV for a single piezoelectric at 15 m/s across a 1 k Ω resistor.

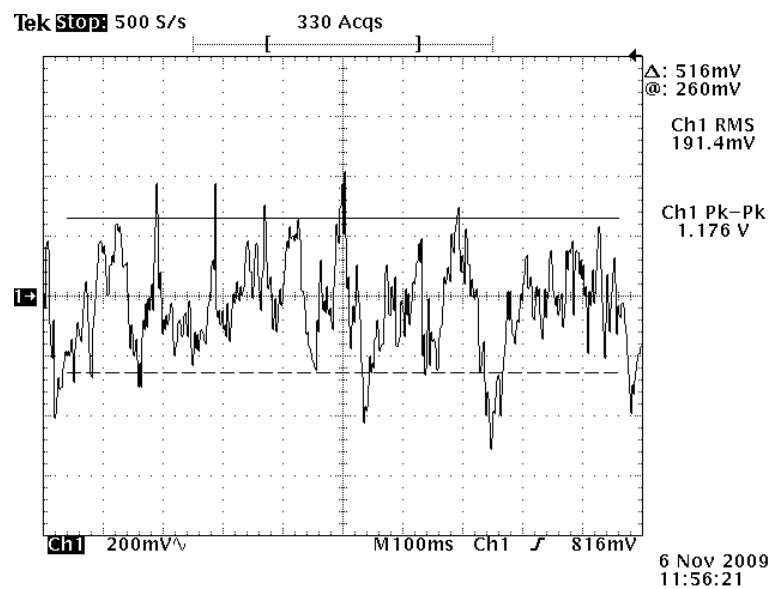


Figure 5.3. OCV for two series piezoelectric elements at 15 m/s.

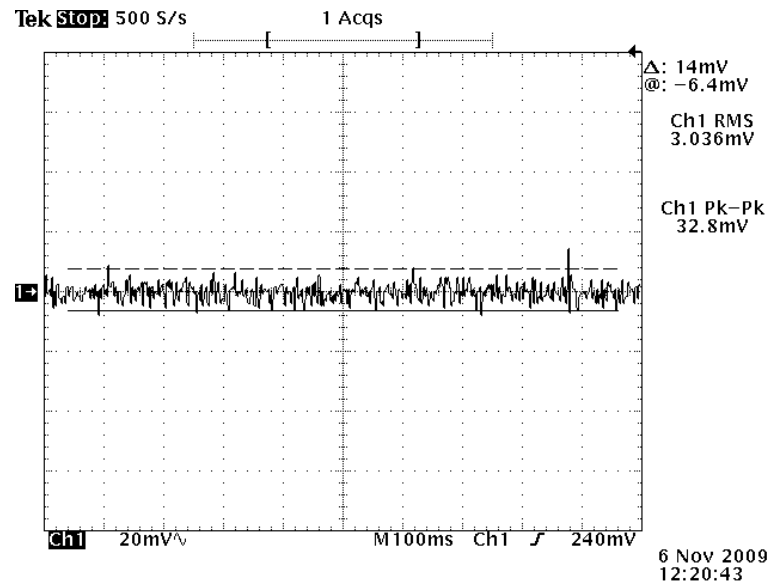


Figure 5.4. CCV for two series piezoelectric elements at 15 m/s across a 1 k Ω resistor.

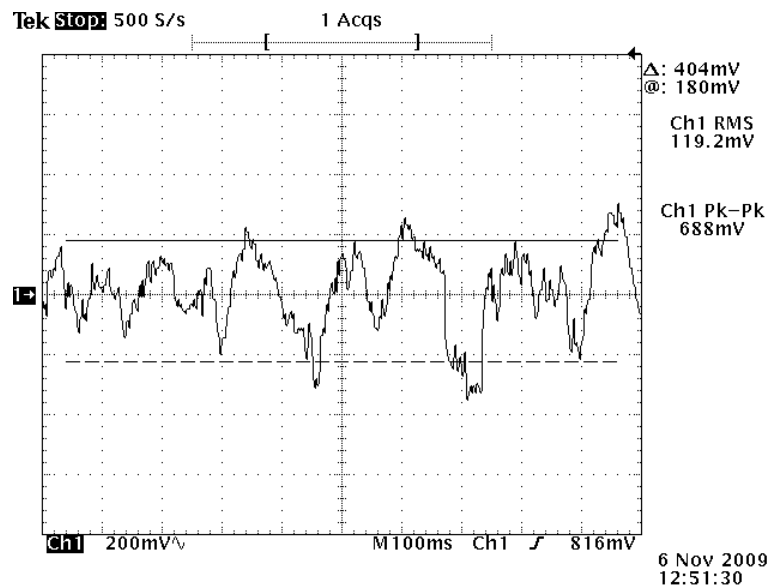


Figure 5.5. OCV for two parallel piezoelectric elements at 15 m/s.

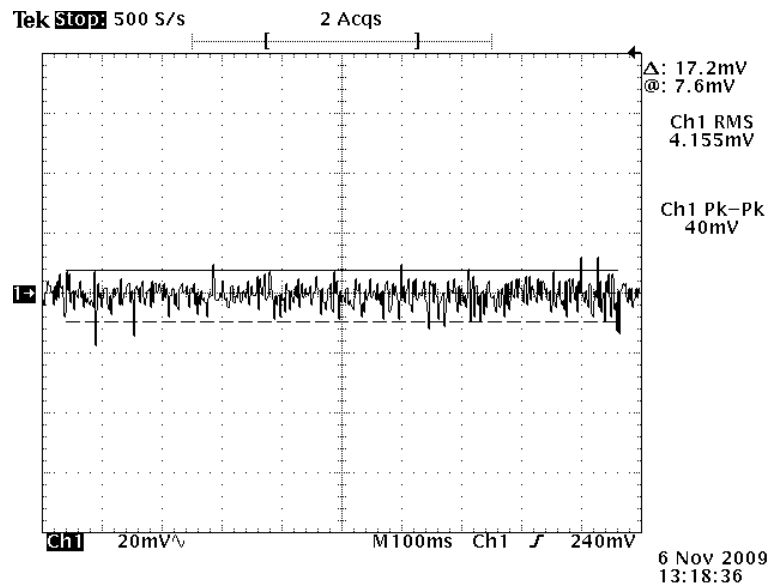


Figure 5.6. CCV for two parallel piezoelectric elements at 15 m/s across a 1 k Ω resistor.

The voltage was highest for the two elements in series. This is logical, as capacitors are similar to voltage sources within a circuit—when in series, voltages are additive; when in parallel, current is additive.

Note that the sample rate here was 500 Hz—much too low to capture all of the signal, as is mentioned in section 5.2.

After viewing these signals with the scope, LabVIEW software and the NI DAQ were used to measure and record air velocity, OCV, and CCV. These results are graphed in Figures 5.7-5.9.

It should be noted that these graphs show the results of measuring the peak-to-peak (PP) OCV and CCC. The sample rate for this first test was 0.25 Hz—too low to draw many conclusions about the material or the test.

However, this initial test showed a number of things. First, the concept of this study is correct; power can be harvested from turbulent airflow using PEG. Second, the voltage and current characteristics were shown to be alternating between positive and negative values, but at no constant frequency. Third, the frequency content was above that which was measured using LabVIEW (0.25 Hz). As such, a much higher sampling rate was used for the road test (see below). Fourth, the relationship between power and air velocity is shown. Figures 5.7 – 5.9 show power as a function of air velocity for the

single piezoelectric element, two elements in series, and two elements in parallel. Power in these figures was obtained by using the OCV and the CCC as measured using LabVIEW. All figures show instantaneous power values calculated from RMS OCV and CCC values. Note that these graphs closely match the power function shown in Figure 3.1.

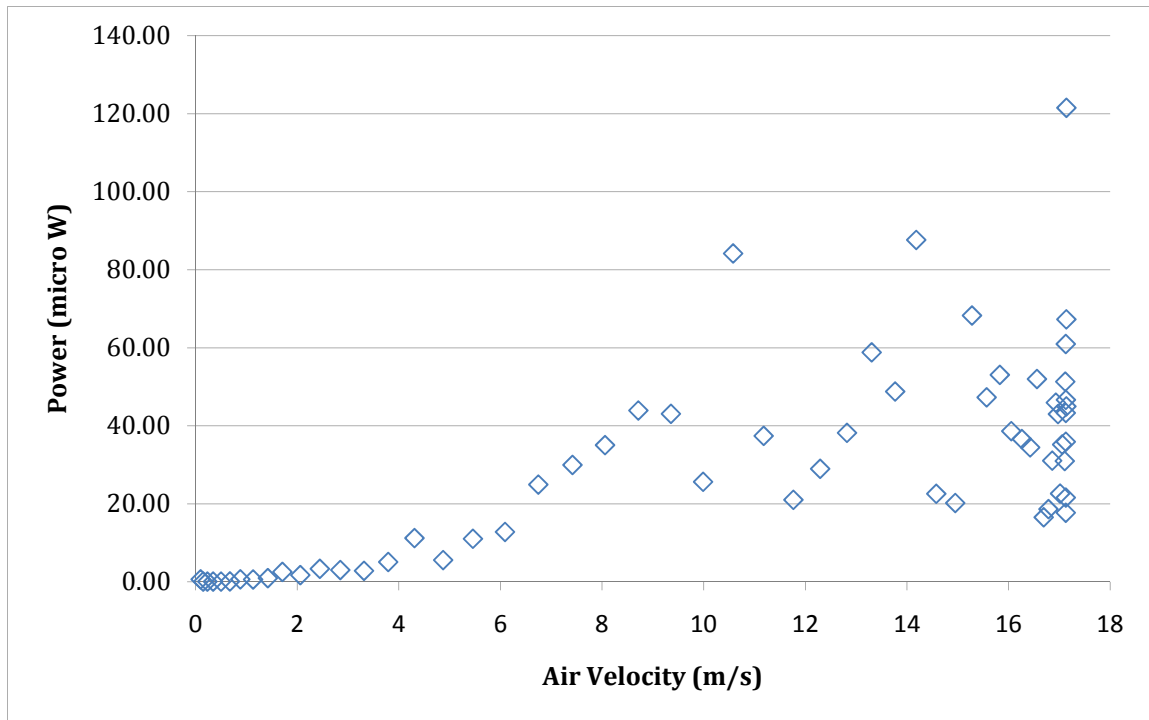


Figure 5.7. Instantaneous power from a single piezoelectric element using LabVIEW.

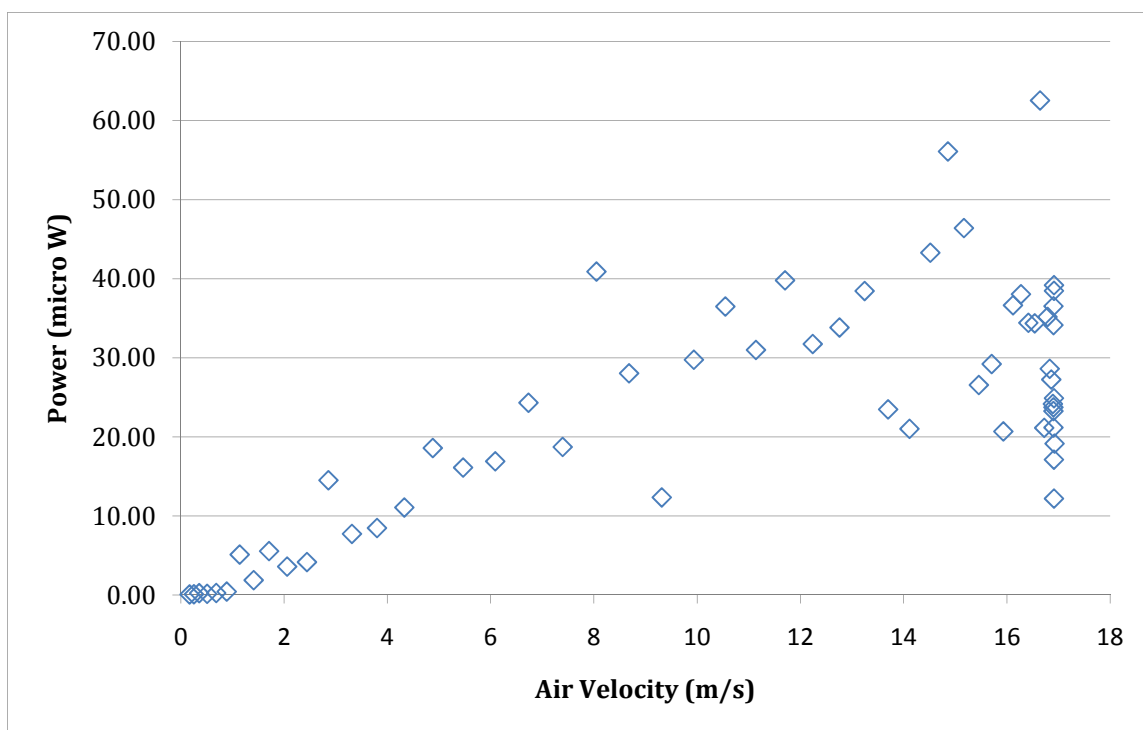


Figure 5.8. Instantaneous power from two series piezoelectric elements using LabVIEW.

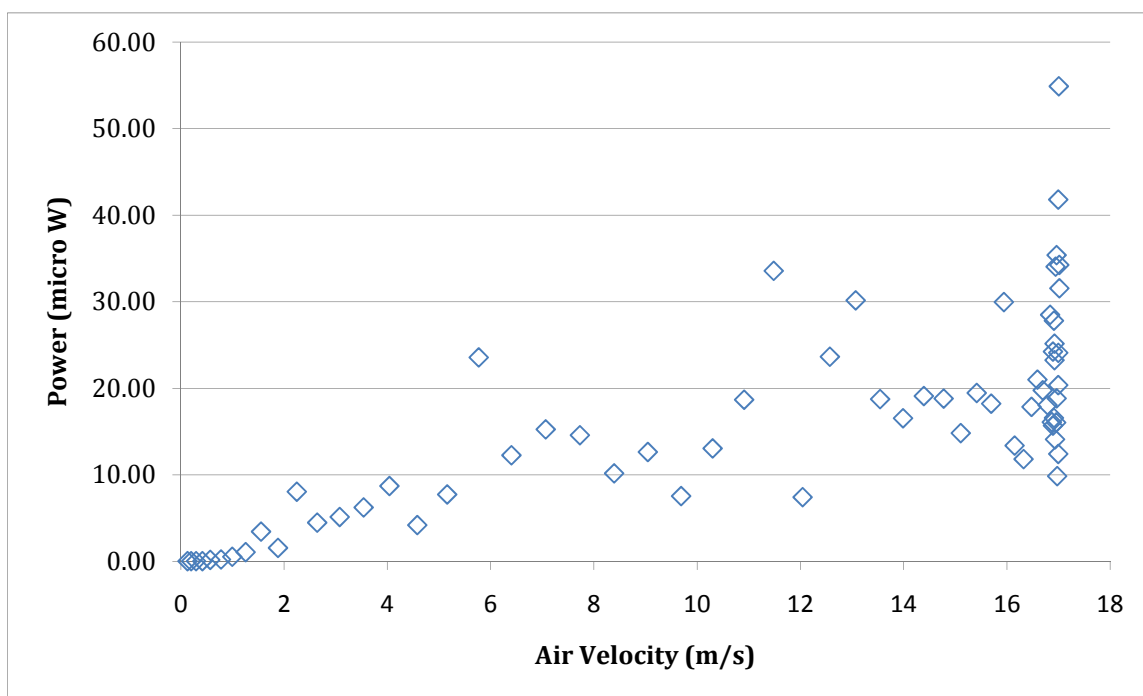


Figure 5.9. Instantaneous power from two parallel piezoelectric elements using LabVIEW.

RMS voltage and current were quite low—not enough to rectify the signal using a diode. It should be noted that higher air velocities would lead to higher forces on the piezoelectric elements and thus higher power. This can be clearly seen from the relationships shown in the figures above.

5.2. Road Test Results

After performing these basic measurements with the bench test, the experiment was then performed using a vehicle on the road. The size and material of the piezoelectric element were the same as in the wind tunnel test. Although more power could have been obtained, as a larger area was possible, it was deemed wise to hold these variables constant.

For each test, the vehicle was brought to above 22 m/s. The data collection then began and the vehicle was brought to a stop. Figure 5.13 shows a representative graph of velocity versus time for one of these tests. There was a 23% variation for this slope between tests. Note that each test run was 30 seconds long.

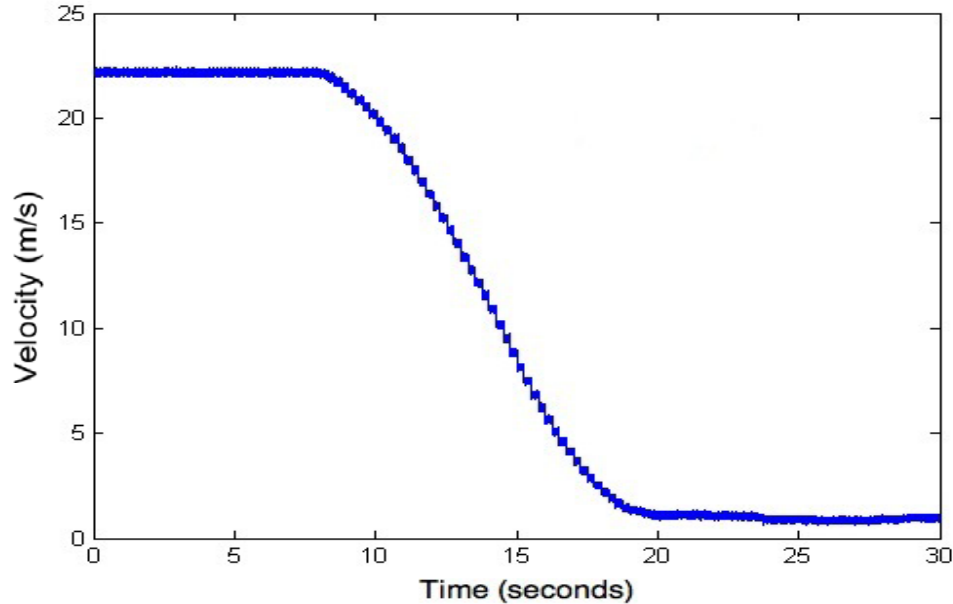


Figure 5.10. Sample velocity vs. time for road test.

As the data previously collected was at the 0.25 Hz range, the sampling rate was increased—first to 4 kHz, then to 20 kHz, and finally to 40 kHz. The OROS DAQ allowed for the measurement of OCV and CCV (across the 1 k Ω resistor) from the piezoelectric element, as well as the frequency content of both these signals. The OROS DAQ had an input range of ± 15 V and a resolution of 16 bits. The CCV was then converted to CCC by dividing by the resistance across which the measurement was taken (1 k Ω).

5.2.1. System Noise

In order to determine the noise in the data, trial runs at 0 m/s were taken to view the frequency content and the noise present. The noise in the system was very low—less than -125 dB/Hz. The frequency content of this test can be seen in Figure 5.14.

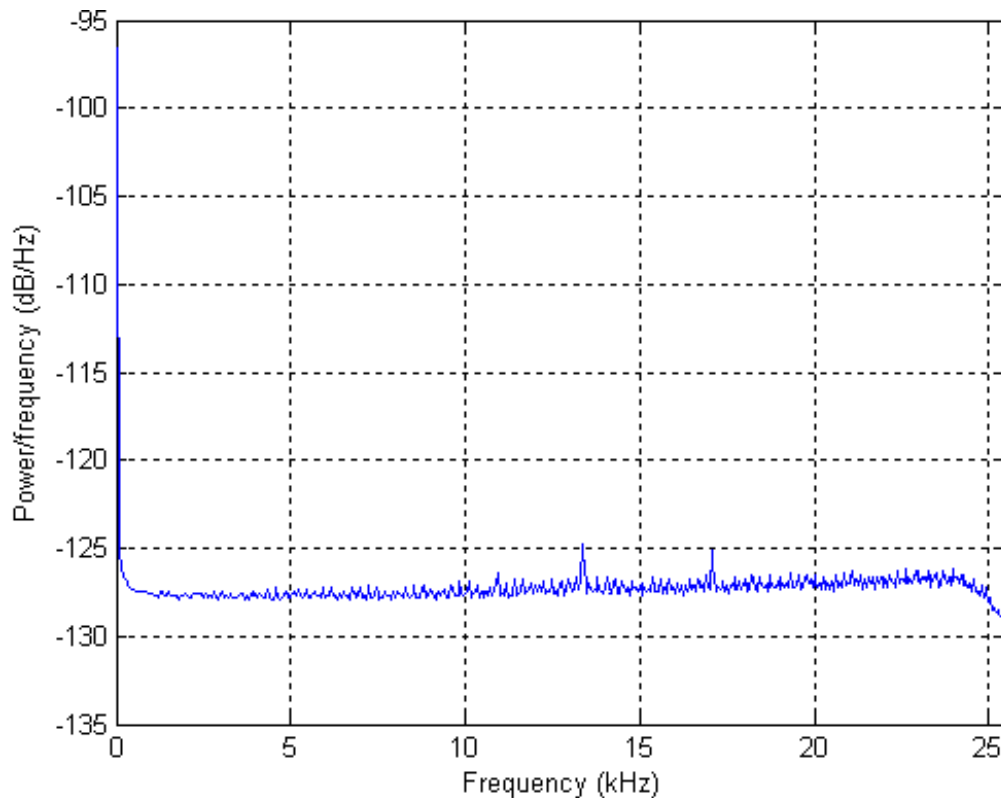


Figure 5.11. Welch power spectral density estimate for OCV from one element at 0 m/s.

5.2.2. Piezoelectric OCV Characteristics

In each of the tests, no voltage was produced below an air velocity of 15 m/s. This can easily be seen as an almost instantaneous drop in voltage. Figure 5.15 shows this effect in detail. Below this velocity, the force of the air upon the element is not enough to generate much measurable voltage. If one were to use a larger or thicker element, this velocity may be expected to increase.

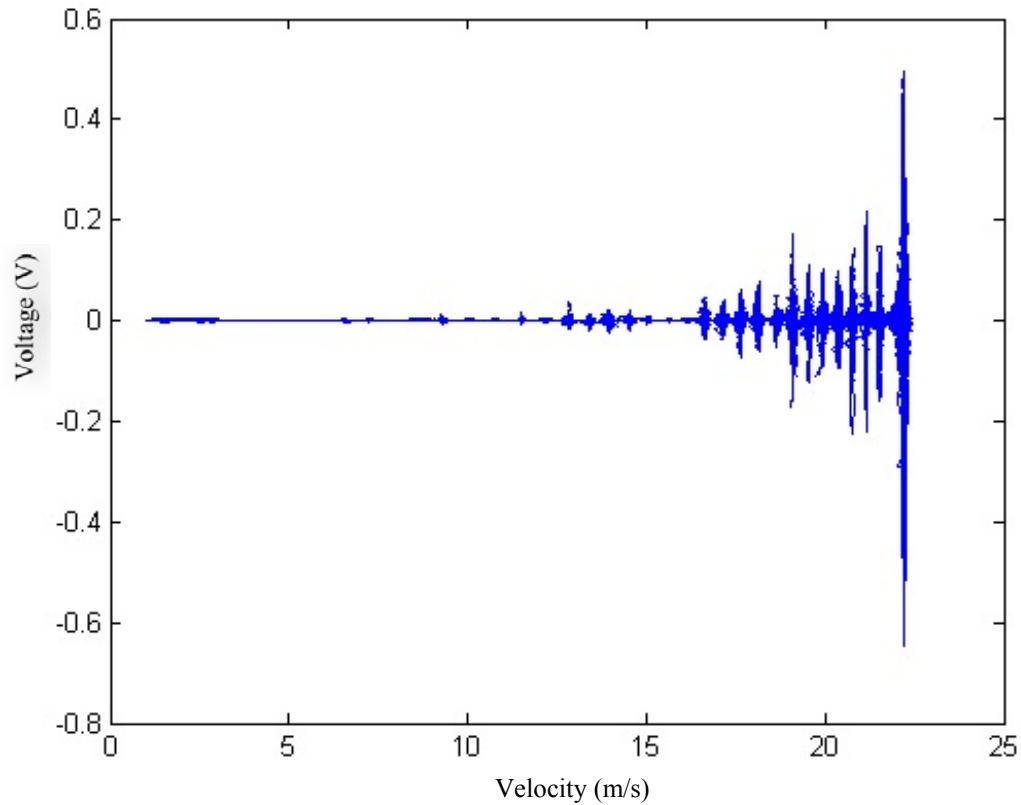


Figure 5.12. OCV vs. velocity for a single piezoelectric element.

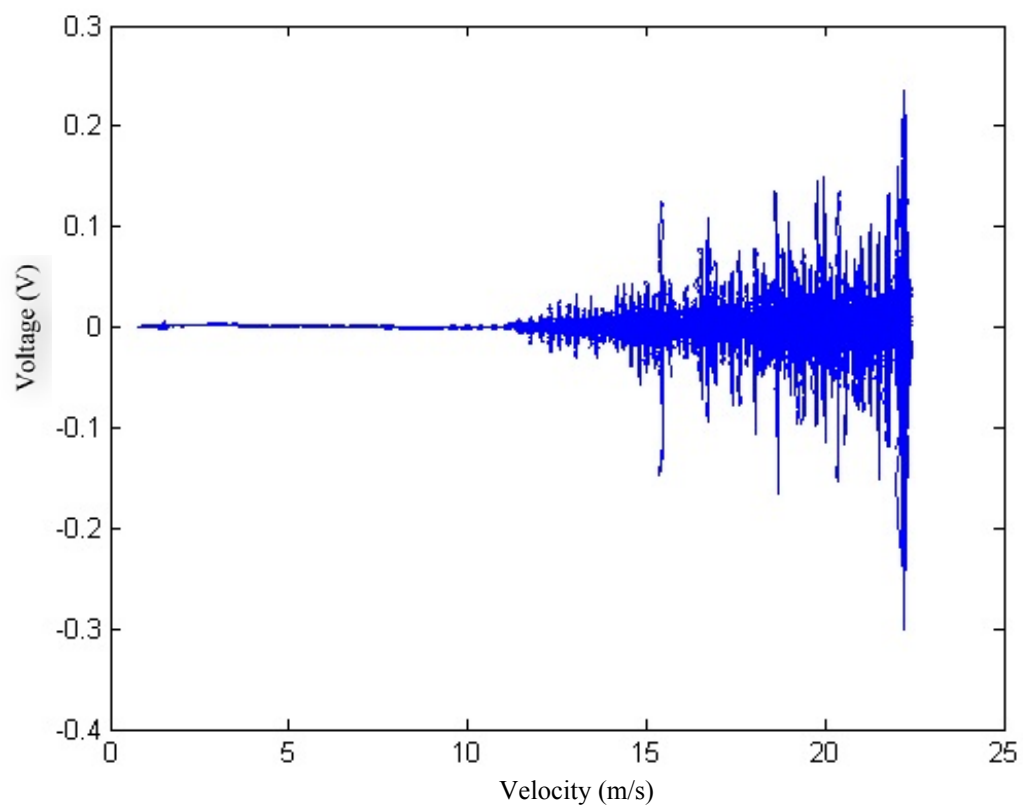


Figure 5.13. OCV vs. velocity for two piezoelectric elements in series.

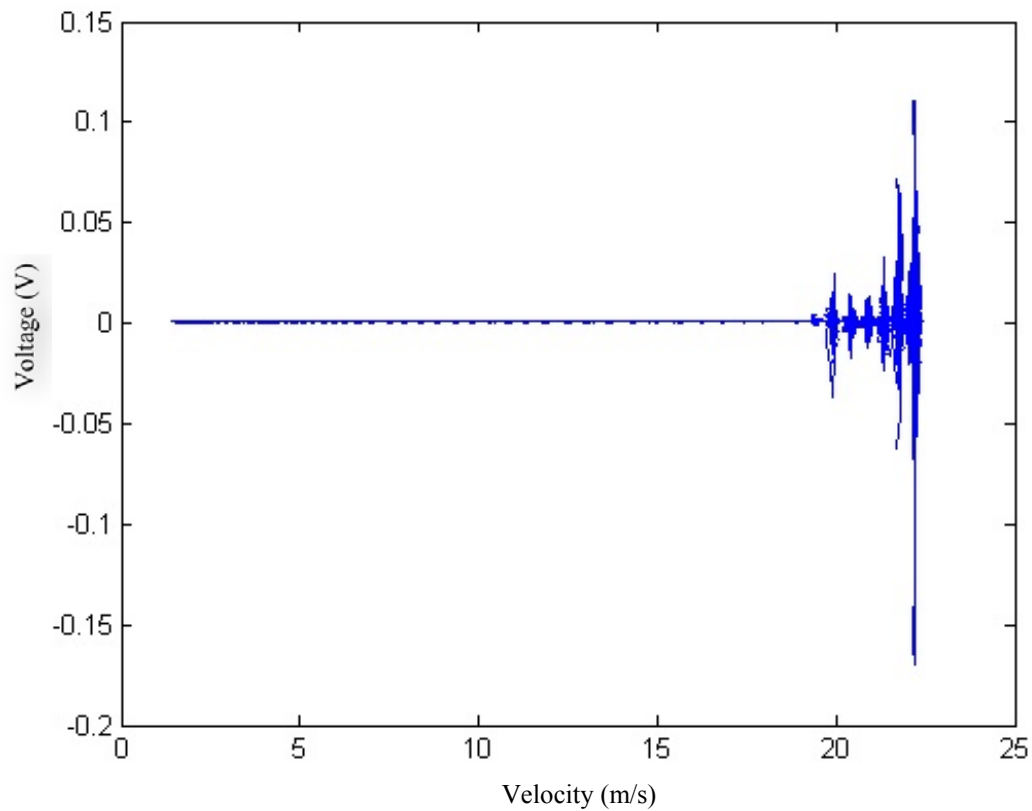


Figure 5.14. OCV vs. velocity for two piezoelectric elements in parallel.

5.2.3. Piezoelectric CCV Characteristics

In order to measure the current output of the piezoelectric element, CCV was measured across a series connected 1 k Ω resistor. The measured values can be seen in Figures 5.18 – 5.20. Once again, as with OCV, very little was observed below an air velocity of 15 m/s.

The spike in voltage shown in Figure 5.18 was a brief increase in air velocity at the end of the test.

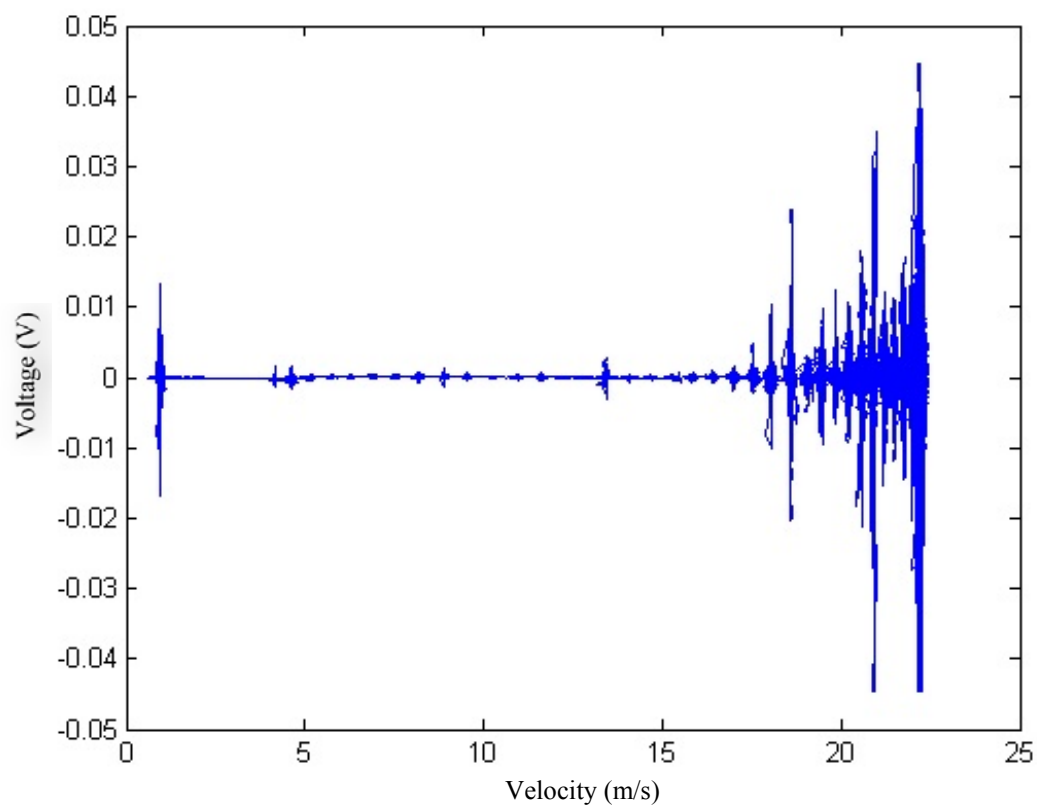


Figure 5.15. CCV vs. velocity for a single piezoelectric element.

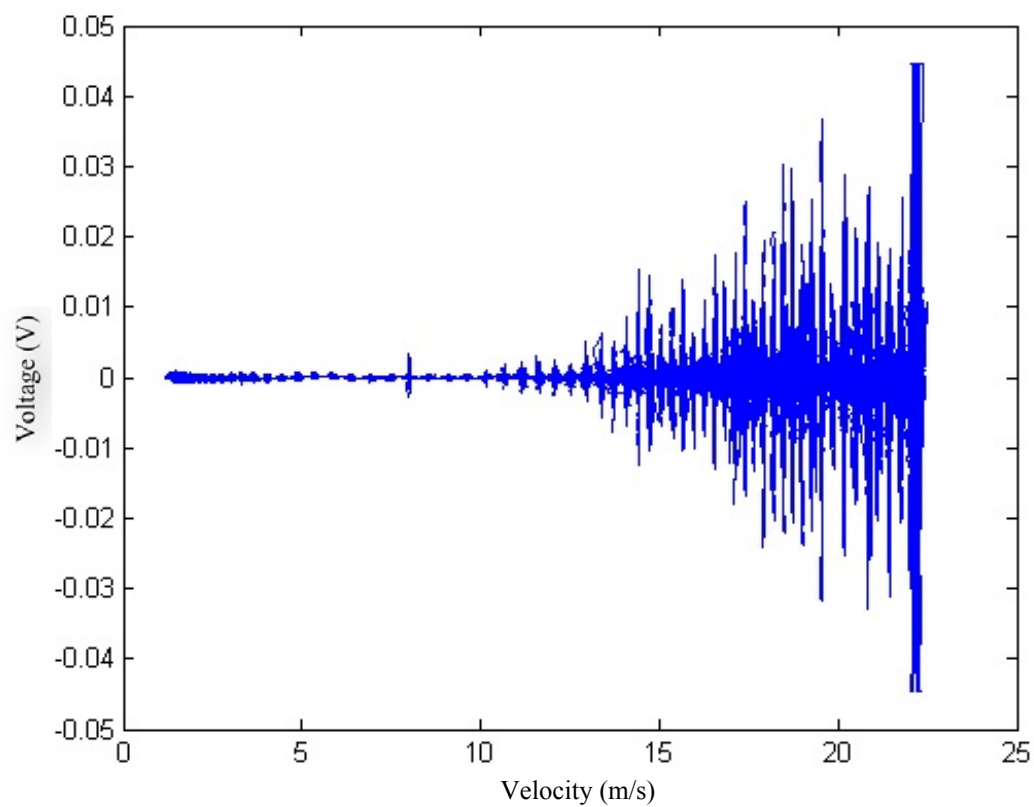


Figure 5.16. CCV vs. velocity for two piezoelectric elements in series.

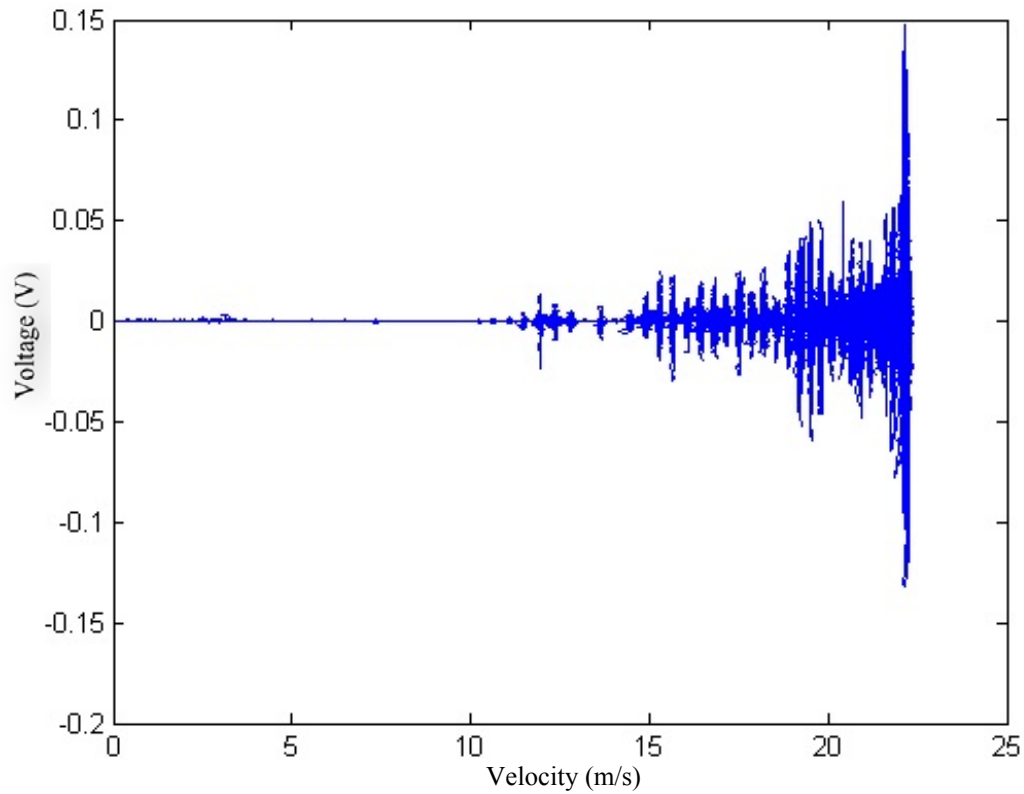


Figure 5.17. CCV vs. velocity for two piezoelectric elements in parallel.

5.2.4. RMS Values

In order to obtain an accurate power output, RMS OCV and CCV were calculated for the portion of the data that had a signal; including the entire trial would have led to erroneously low RMS values. RMS values for OCV, CCC, and power for each of the three test set-ups are shown in Table 5.1.

Table 5.1. OCV and calculated RMS, CCC, and power values.

Arrangement	OCV (V)	CCC (A)	Power (W)
1 Piezo	1.96E-02	2.80E-06	5.49E-08
2 Series	1.22E-02	2.30E-06	2.81E-08
2 Parallel	3.50E-03	6.40E-06	2.24E-08

While proving that the concept works, these numbers do not come close to the aforementioned target of 20 mW.

5.2.5. Voltage Frequency Characteristics

Perhaps one of the most interesting facets of this study was the frequency generated by the piezoelectric element. It was the original thought of the author that these frequencies generated would be rather low (less than 1 kHz), due to the fact that it is difficult for a physical object of this size to oscillate at high frequencies. However, as can be seen in Figure 5.16, there was a large portion of high-frequency voltage with a distinct spike at 3.5 kHz.

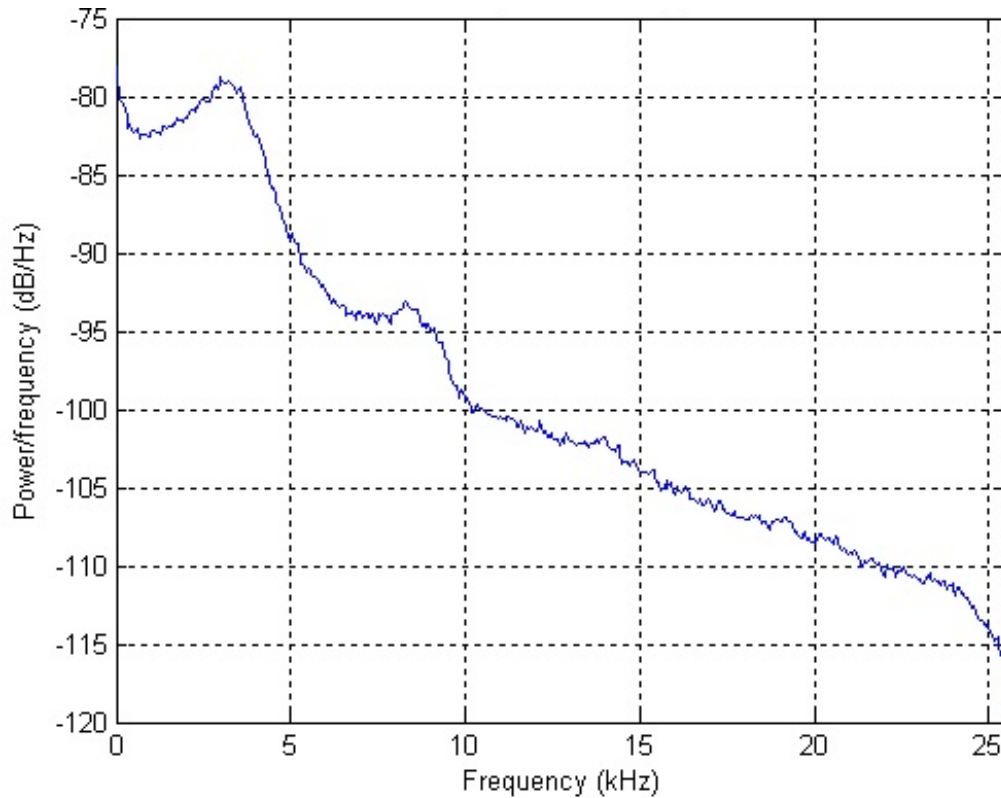


Figure 5.18. Welch power spectral density estimate for a single element.

The same was found to be true in all three cases. Although this spike was shifted slightly for the case with two elements in series to 2.5 kHz (Figure 5.19), this was still

higher than the expected. This change in frequency may have multiple sources. One could be that one element's output was cancelled by the other's, thereby reducing the content at that particular frequency. This possibility is further discussed in section 5.3.

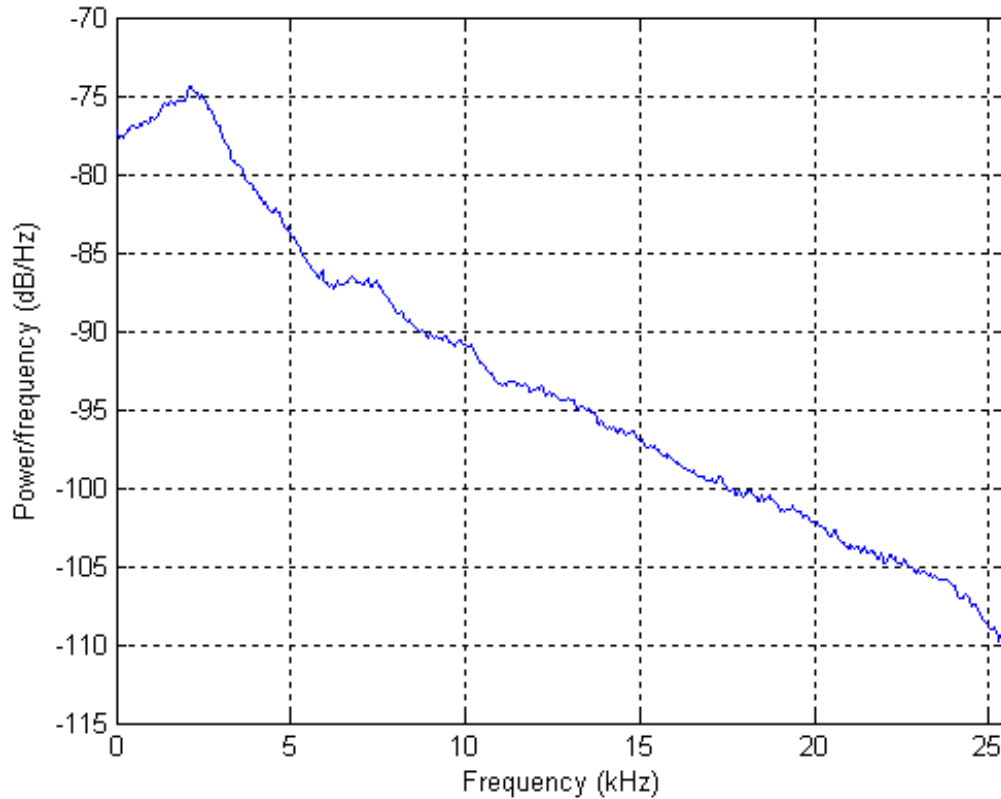


Figure 5.19. Welch power spectral density estimate for two elements in series.

It should also be noted that although each of the power spectral density figures have a similar shape, the quantity of frequencies present in each changed. For example, for the single piezoelectric element, the frequency content was about -79 dB/Hz at resonance (Figure 5.18). Compare this to the series combination, -75 dB/Hz (Figure 5.19), and the parallel combination, -90 dB/Hz (Figure 5.20).

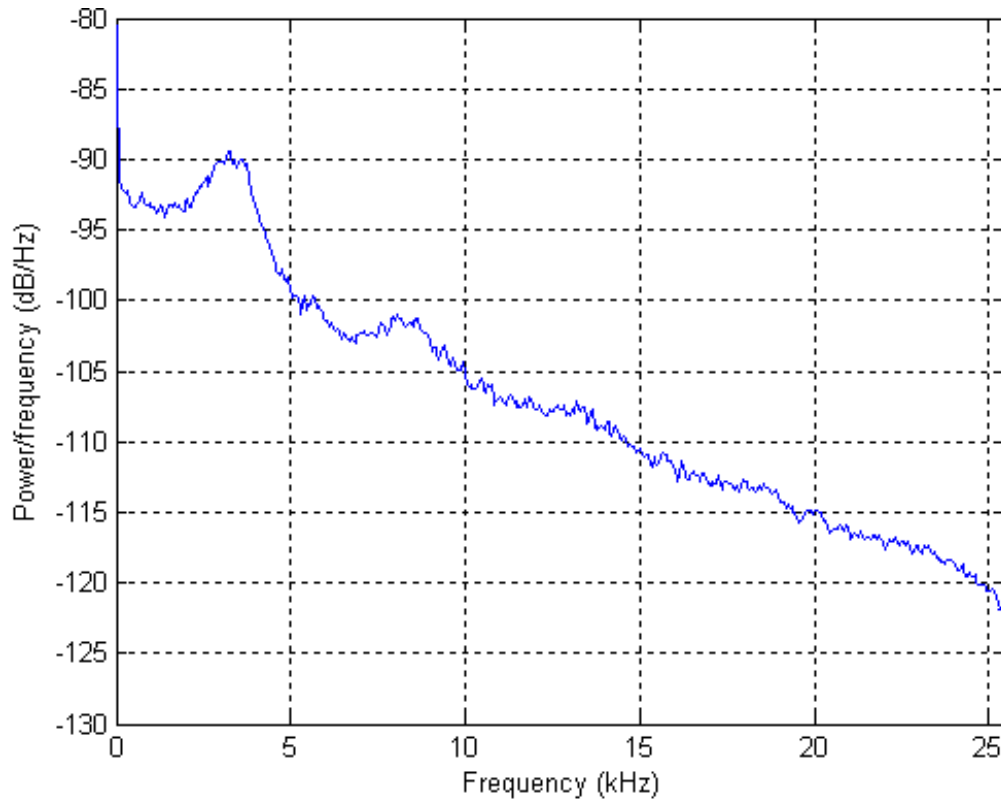


Figure 5.20. Welch power spectral density estimate for two elements in parallel.

This high-frequency power content has a few possible explanations. First, as the force applied by the air was randomly changing, the voltage produced by the piezoelectric element was randomly changing. These random and rapid changes lead to higher frequency content. Second, although this study was focused on horizontal, flag-type motion, there were other stresses being applied to the element. For example, there may have been force components that applied tension to the flag along both its vertical and horizontal axes. There may have been compressive forces, as well.

These forces combined could have produced frequencies much higher than the simple flapping that was assumed here. Future study may be focused on which of these components contributed the most to power generation and how to maximize this affect.

In order to determine whether this was indeed physically possible, the piezoelectric element was then attached to a function generator. A Wavetek 182A was used. This device had the capabilities of producing frequencies from 0.004 Hz to 4 MHz.

The function generator was first attached to a scope to check its accuracy. After this was confirmed, the piezoelectric element was attached to the function generator. A 20 V PP signal was sent to the piezoelectric element. The frequency of this signal was adjusted. Although no physical movement was visible, the vibrations produced were audible. Frequencies as high as 1.7 kHz could be easily heard, indicating that vibrations at these high levels are possible. These vibrations, however, were not the flag-type movement discussed here, but some form of compressive and tensile forces, perhaps along the element's horizontal axis.

5.3. Series & Parallel Circuit Issues

Although voltage should be additive when the elements are in series, and thus approximately twice as large as the single element values, the data does not reflect this. In fact, the single piezoelectric element produced the largest RMS voltage and power. The OCV voltage for the two elements in series was only 62% of the single element's voltage. This could be caused by the elements bending in opposite directions, producing voltages of opposing signs, and thus canceling each other.

In the case of CCC, the two elements in parallel did produce what was expected—approximately twice as much current as the single piezoelectric element (229%). However, the voltage here was lower by 83%. This could also be due to the aforementioned cancelling effect.

5.4. Power Considerations

The power produced by the piezoelectric is not the only concern. Power density is an important consideration as well. As the piezoelectric flag could be considered a two-dimensional object if thickness is ignored, the following equation gives the maximum power density per unit area:

$$P_D = P_{MEAS} / A, \quad (\text{Eq. 5.1})$$

where P_D is the power density (W/m^2), P_{MEAS} is the experimentally measured piezoelectric power output (W), and A is the area of the piezoelectric element (m^2). Note that the area of one piezoelectric element was 0.00638 m^2 . Using the data obtained from

the road test, power density for the single piezoelectric was the highest at $8.61 \mu\text{W}/\text{m}^2$. The power densities of the series and parallel combinations were $2.20 \mu\text{W}/\text{m}^2$ and $1.76 \mu\text{W}/\text{m}^2$, respectively. The data for these calculations can be found in Table A-2 in the Appendix.

Efficiency of the element can be found as:

$$\eta = P_{\text{MEAS}} / P_{\text{PEG}}, \quad (\text{Eq. 5.2})$$

where η is the efficiency of the element in question and P_{PEG} is the theoretical maximum power for this setup. The single piezoelectric element yielded the highest numbers, with an efficiency of $1.08 \times 10^{-6} \%$. The series combination had an efficiency of $5.54 \times 10^{-7} \%$. The parallel combination had an efficiency of $4.42 \times 10^{-7} \%$.

The micro-scale efficiencies are due in part to the fact that the maximum power was calculated at a constant air velocity, whereas the RMS values mentioned here were measured at decreasing air velocities. In addition, although the overall velocity as measured was as high as 22 m/s, the nature of turbulence dictates that some of the velocity components acting on the piezoelectric material were lower. Therefore, the forces acting on the piezoelectric were smaller than the estimated theoretical maximum.

Another possibility is due to the nature of the piezoelectric material. When a force is applied to a piezoelectric material in one direction, a voltage of a certain magnitude and sign is created. If a force of the same magnitude but the opposite direction is placed on the piezoelectric material, a voltage of the same magnitude as before, but with the opposite sign, will be produced. A piezoelectric material that is flapping (such as the ones used in this study) is undergoing various forces in various directions. It is possible that some of these forces are opposing others. Thus, voltages produced may cancel each other out before they leave the material.

Although power produced by the wind tunnel seemed to be higher, this power was calculated on an instantaneous basis, thus taking into account the PP values, rather than the RMS. The data, therefore, show much higher power generated.

5.5. Effect on Drag

The actual effect on drag was not determined. Three possibilities exist: increase, no influence, or decrease. Although it may seem that this will add drag to the overall design, this is not necessarily the case. Regardless of whether the energy is captured or not, the moving body must give up energy to the air in order to move it. Once the air passes the body, there is still energy present in the form of turbulence. This turbulence adds to the overall aerodynamic drag. If this turbulence were to be reduced, the overall drag will also decrease. Thus, harvesting energy from the wind has the two-fold possibility of making useable electric power as well as reducing drag.

CHAPTER 6. CONCLUSIONS

In light of rising energy costs and increasing demand, new technologies such as PEG can be of great benefit. Research surrounding these may lead to new sources for energy harvesting. In addition, the flexibility and simplicity of PEG allow for installation in areas where other generation techniques might not be feasible.

The technique used in this research generated acceptable voltage. Although small, this voltage could be used for other applications, had the current generated been high enough. The nature of the piezoelectric element, as a capacitive device, lends itself to small current generation.

Based on the null and alternative hypotheses set forth at the beginning of this experiment, this application did not yield enough power to meet the requirements. The null hypothesis— H_0 : No useable power can be harvested from this setup—cannot be rejected based on this data. To remind the reader, no statistical analysis was used for this evaluation, as this was a quasi-experimental study (see section 1.5).

Although the power produced did not meet the 20 mW requirement, a few phenomena were observed. First, the chaotic AC nature of the piezoelectric voltage was observed. These observations would be useful in future studies, as the signal would need to be rectified in order to be of much use in this application. To this end, more efficient rectification techniques would be needed. Second, although adding multiple piezoelectric elements in series or parallel seemed to be a good solution to low power production, this only exacerbated the problem. As the voltages varied, they often cancelled each other out, producing a lowered voltage. Thus, as above, an efficient rectification technique would be required before combining the signals. After this, however, the signals could be combined for increased output. Third, the frequency content of the voltage signal was quite high. This may be looked at as a positive or a negative finding; in many instances it

is easier to produce high frequency forces. However, in wind applications, it is often low frequency forces that produce much power.

The findings here could make a basis for future study. Rectification for PEG is a topic studied by many researchers, but there is still much work to be done in this area. More efficient rectification techniques would lead to more usable power, as the signals could be rectified first and then combined.

Further investigation of the dynamic interaction between the piezoelectric element and the air currents could also lead to interesting developments. A study on placement and the effect on aerodynamic drag would be of great help were one to attempt to further this technology. As more turbulent flow is present in some areas than others (under the vehicle and behind it), the placement could be varied to observe power output and the effect on the drag coefficient.

In addition to placement, it would be interesting and helpful to view the various forces acting on the piezoelectric element within the flow. By doing this, one could more accurately predict the maximum amount of power harvestable. This may also lead to a better understanding of the interaction between the element and the flow. In order for this to be of much use, a large number of sensors would be required, as well as a more sophisticated DAQ system.

Another possibility for future study would be the use of other types of piezoelectric materials. While the k_{33} constant for PVDF is 12%, other materials have much higher k_{33} values; one such material is PZT, which has a k_{33} of around 70%. This would lead to higher power output.

Future study could also investigate the relationship of power and velocity shown here. Although this relationship seems generalizable to higher velocities, there may be findings otherwise at much higher velocities. In general, higher velocities will lead to higher forces on the piezoelectric element, which should lead to higher voltage, current, and power output.

The limited current understanding of turbulent flow also is an interesting aspect of this study. No current research allows one to compute the amount of energy in a given turbulent situation. As such, it is difficult to quantify the theoretical maximum power

harvestable in a situation such as this. As mentioned in Chapter 5, this could be part of the reason for the low efficiencies found here.

BIBLIOGRAPHY

BIBLIOGRAPHY

- Dong, Shuxiang, Li, J. F., Viehland, D., Cheng, J., Cross, L. E. (2004). A Strong Magnetoelectric Voltage Gain Effect in Magnetostrictive-piezoelectric Composite. *Applied Physics Letters*, 85, 3534-3536.
- Dong, Shuxiang, Li, Jie-Fang, Viehland, D. (2006). Magnetoelectric coupling, efficiency, and voltage gain effect in piezoelectric-piezomagnetic laminate composites. *Journal of Materials Science*, 41, 97-106.
- Friedmann, H., Petricevic, R., Ries, M. (2007). On the way to active systems: AVR Rotor – active vibration reduction for a textile bobbin. *Computers and Structures*, 86, 447-453.
- Funasaka, Tsukasa, Furuhashi, Makoto, Hashimoto, Yasuharu, & Nakamura, Kiyoshi. (1998). Piezoelectric Generator Using a LiNbO₃ Plate with an Inverted Domain. *IEEE Ultrasonics Symposium*, 1998, 959-962.
- Gillespie, Thomas D. (1992). *Fundamentals of Vehicle Dynamics*. Society of Automotive Engineers (1992) Warrendale, PA.
- Grove, T. T., Ehle, A. (2002). Impulse, momentum, and energy of human strikes using inexpensive piezo disks. *American Journal of Physics*, 72, 281-284.
- Jifeng Han, Annette von Jouanne, Triet Le, K. Mayaram, T. S. Fiez. (2003). Novel Power Conditioning Circuits for Piezoelectric Micro Power Generators. Applied Power Electronics Conference and Exposition, 2004. APEC '04. *Nineteenth Annual IEEE*, 3, 1541- 1546.
- Kim, Sunghwan. (2002). Low power energy harvesting with piezoelectric generators (Doctoral dissertation, University of Pittsburgh, 2002). *Dissertation Abstracts International*, 64/02, 920.
- Kim, Sunghwan, Clark, William W., & Wang, Qing-Ming. (2005). Piezoelectric Energy Harvesting with a Clamped Circular Plate: Analysis. *Journal of Intelligent Material Systems and Structures*, 16, 847-854

- Lu, F., Lee, H. P., & Lim, S. P. (2002). Modeling and analysis of micro piezoelectric power generators for micro-electromechanical-systems applications. *Smart Materials and Structures*, 13, 57-63.
- Makihara, Kanjuro, Onoda, Junjiro, & Minesugi, Kenji (2006). Behavior of Piezoelectric Transducer on Energy-Recycling Semiactive Vibration Suppression. *AIAA Journal*, 44, 411-413.
- Ogando, Joseph (2007, June 25). Adaptronic Vibration Control. *Design News*, 2007, June, 33-35.
- Ottman, Geoffrey K., Hofmann, Heath F., and Lesieutre, George A.. (2003). Optimized Piezoelectric Energy Harvesting Circuit Using Step-Down Converter in Discontinuous Conduction Mode. *IEEE Transactions on Power Electronics*, 18, No. 2.
- Poulin, G., Sarraute, E., & Costa, F. (2003). Generation of electrical energy for portable devices Comparative study of an electromagnetic and a piezoelectric system. *Sensors and Actuators, A* 116, 461-471.
- Priya, Shashank. (2007). Advances in energy harvesting using low profile piezoelectric transducers. *Journal of Electroceramics* (2007), 19:165-182
- Ramsey, M.J. and Clark, W.W. 2001. "Piezoelectric Energy Harvesting for Bio MEMS Applications," *Proceedings of SPIE's 8th Annual Smart Materials and Structures Conference*, Newport Beach, CA, 4332-2001, 429-438.
- Richard, C., Guyomar, D., Audigier, D., and Bassaler, H., "Enhanced Semi Passive Damping Using Continuous Switching of a Piezoelectric Device on an Inductor," *Proceedings of the SPIE Smart Structures and Materials Conference*, 3989, Society of Photo-Optical Instrumentation Engineers, Bellingham, WA, 2000, 288-299.
- Roundy, S. and Wright, P. K. (2004). A piezoelectric vibration based generator for wireless electronics. *Smart Materials and Structures*, 13, 1131-1142.
- Sekaran, Uma. (2002). *Research Methods for Business: A Skill Building Approach* (2002) New York, NY.
- Smith, W. A., Shaulov, A. A., Singer, B. M. (1984). Properties of composite piezoelectric materials for ultrasonic transducers. *Ultrasonics Symposium*, 1984, 539-544.
- Sodano, Henry A., Inman, Daniel J., Park, Gyuhae (2005). Generation and Storage of Electricity from Power Harvesting Devices. *Journal of Intelligent Material Systems and Structures*, 16, 67-75.

- Song, Hyun-Cheol, Kim, Hyung-Chan, Kang, Chong-Yun, Kim, Hyun-Jai, Yoon, Seok-Jin, & Jeong, Dae-Yong (2007). Multilayer piezoelectric energy scavenger for large current generation. *Journal of Electroceramics*, 23, 301-304.
- Starner, T. 1996, "Human-Powered Wearable Computing," *IBM Systems Journal*, 35:618-629.

APPENDIX

APPENDIX

Table A-1. *Maximum power data.*

Drag coeff.	Air density	Velocity	Piezo area	Vehicle frontal area	Drag force on vehicle	Drag force at sides (10%)	Turbulent drag force acting on piezo	Max. power at sides	Max. power with Betz limit	Max. power with k_{33} (12%)
C_D	ρ (kg/m ³)	v (m/s)	A_{PEG} (m ²)	A (m ²)	F (N)	(N)	(N)	(W)	(W)	(W)
1.05	1.233	2.00	0.00638	0.14790	0.3831	0.0383	0.0008	0.0017	0.0010	0.0001
1.05	1.233	4.00	0.00638	0.14790	1.5324	0.1532	0.0033	0.0132	0.0078	0.0009
1.05	1.233	6.00	0.00638	0.14790	3.4478	0.3448	0.0074	0.0446	0.0265	0.0032
1.05	1.233	8.00	0.00638	0.14790	6.1294	0.6129	0.0132	0.1058	0.0627	0.0075
1.05	1.233	10.00	0.00638	0.14790	9.5772	0.9577	0.0207	0.2066	0.1225	0.0147
1.05	1.233	12.00	0.00638	0.14790	13.7912	1.3791	0.0297	0.3569	0.2117	0.0254
1.05	1.233	14.00	0.00638	0.14790	18.7713	1.8771	0.0405	0.5668	0.3361	0.0403
1.05	1.233	16.00	0.00638	0.14790	24.5176	2.4518	0.0529	0.8461	0.5017	0.0602
1.05	1.233	18.00	0.00638	0.14790	31.0301	3.1030	0.0669	1.2047	0.7144	0.0857
1.05	1.233	20.00	0.00638	0.14790	38.3088	3.8309	0.0826	1.6525	0.9800	0.1176
1.05	1.233	22.00	0.00638	0.14790	46.3536	4.6354	0.1000	2.1995	1.3043	0.1565
1.05	1.233	24.00	0.00638	0.14790	55.1647	5.5165	0.1190	2.8556	1.6934	0.2032
1.05	1.233	26.00	0.00638	0.14790	64.7419	6.4742	0.1396	3.6306	2.1530	0.2584
1.05	1.233	28.00	0.00638	0.14790	75.0852	7.5085	0.1619	4.5346	2.6890	0.3227
1.05	1.233	30.00	0.00638	0.14790	86.1948	8.6195	0.1859	5.5773	3.3073	0.3969
1.05	1.233	32.00	0.00638	0.14790	98.0705	9.8071	0.2115	6.7688	4.0139	0.4817

Table A-2. *Piezoelectric element efficiency.*

Arrangement	Power Generated (W)	Power Density (W/m ²)	Maximum Theoretical Power Harvestable (W)	Efficiency (%)
Single Piezoelectric	5.49E-08	8.61E-06	5.07E-02	1.08E-06
Series Piezoelectric	2.81E-08	2.20E-06	5.07E-02	5.54E-07
Parallel Piezoelectric	2.24E-08	1.76E-06	5.07E-02	4.42E-07